

RESEARCH

Nutrient and Trace Element Contributions from Drained Islands in the Sacramento–San Joaquin Delta, California

Christina M. Richardson*¹, Joseph K. Fackrell^{1,2}, Tamara E. C. Kraus², Megan Young³, Adina Paytan⁴

ABSTRACT

Inventorying nutrient and trace element sources in the Sacramento-San Joaquin Delta (the Delta) is critical to understanding how changes—including alterations to point source inputs such as upgrades to the Sacramento Regional Wastewater Treatment Plant (SRWTP) and landscape-scale changes related to wetland restoration—may alter the Delta’s water quality. While island drains are a ubiquitous feature of the Delta, limited data exist to evaluate island drainage mass fluxes in this system. To better constrain inputs from island drains, we measured monthly discharge along with nutrient and trace element

concentrations in island drainage on three Delta islands and surrounding rivers from June 2017 to September 2018. These data were used to calculate island-level fluxes and then upscaled to estimate Delta-wide contributions from island drains. Based on these results, we present (1) new estimates of gross and net nutrient and trace element fluxes from Delta island drains, and (2) concomitant N stable isotope data to improve our understanding of island N cycling. Over 60% of nearly all island drainage gross nutrient and trace element loads occurred in winter and spring. Upscaled island drainage net annual total nitrogen (TN), total dissolved nitrogen (TDN), and NH_4^+ loads comprised an estimated 9%, 7%, and 4%, respectively, of annual inputs to this system in 2018, before the SRWTP upgrade. Under a post-upgrade scenario, we estimated net annual island drainage TDN contributions to increase to 11% and NH_4^+ contributions to 45% of total Delta inputs as the SRWTP NH_4^+ load diminished to near zero. Our results suggest that island drainage is a measurable N source that has likely become increasingly important now that the SRWTP upgrade is complete. With over 200 potential active outfalls, these inputs may affect aquatic biogeochemical cycling in many regions of the Delta, especially in areas with long residence times.

SFEWS Volume 20 | Issue 2 | Article 5

<https://doi.org/10.15447/sfeWS.2022v20iss2art5>

* Corresponding author: cmrichar@ucsc.edu

- 1 University of California, Santa Cruz
Earth and Planetary Sciences
Santa Cruz, CA 95064 USA
- 2 US Geological Survey
California Water Science Center
Sacramento, CA 95819 USA
- 3 US Geological Survey
Water Mission Area Laboratory and
Analytical Services Division
Menlo Park, CA 94025 USA
- 4 University of California, Santa Cruz
Institute of Marine Sciences
Santa Cruz, CA 95064 USA

KEY WORDS

Drainage water quality, agricultural drainage, return flow, diversions, Delta island groundwater, nitrogen, phosphorous, metals

INTRODUCTION

Over the last 4 decades, the San Francisco Bay and Sacramento-San Joaquin Delta (the Delta) have experienced drastic ecological changes. From the 1970s to the 1990s, primary production and phytoplankton biomass decreased by 40% and 60%, respectively (Jassby 2008). More recent work shows that chlorophyll *a* concentrations have declined by over 70% since 1975 (Cloern 2019). At the same time, less desirable phytoplankton species that produce cyanotoxins, like *Microcystis*, are increasing in abundance (Lehman et al. 2013). The introduction of a number of invasive species, including two clams, *Potamocorbula amurensis* and *Corbicula fluminea*, are commonly thought of as important catalysts of structural ecological change in this system, and many studies suggest that their introductions have led to at least some of the observed declines in phytoplankton biomass as a result of high grazing rates (Jassby 2008; Jassby et al. 2002). Winder and Jassby (2011) showed zooplankton community shifts over a 37-year period and associated this shift with the clam invasion. Other invasive species, including several aquatic macrophytes (e.g., *Eichhornia crassipes*, water hyacinth, and *Ludwigia hexapetala*, water primrose), persist in the Delta today and are affecting both habitat and water quality (Dahm et al. 2016; Ta et al. 2017).

Higher trophic-level species have experienced similar widespread declines. Decreases over the past 2 decades in pelagic fish abundance, often referred to as Pelagic Organism Decline, have prompted a number of food web studies (Sommer et al. 2007). However, master controls on biomass and production trends remain elusive, likely owing to the hydrologic and biogeochemical complexity of the estuary. While no one variable has been able to fully account for the previously discussed changes, water quality, especially nutrient availability, remains an important control on ecosystem function in estuaries

worldwide (Howarth et al. 2011; Paerl et al. 1998; Paerl et al. 2006; Seitzinger and Sanders 1997).

A number of studies have attempted to assess the effects of nutrient forms and ratios on primary productivity in the Delta environment (see reviews by Senn and Novick [2014]; Dahm et al. [2016]; Ward and Paerl [2016]). Most research on nutrients in the Delta has focused on nitrogen (N) biogeochemistry because of both its ubiquitous presence in human-affected watersheds and because of the widely debated importance of N speciation for primary production in the Delta (Cloern 2021; Kraus et al. 2017; Ward and Paerl 2016). Cloern (2019) showed that ammonium (NH_4^+) and nitrate plus nitrite ($\text{NO}_3^- + \text{NO}_2^-$) concentrations in the Delta have changed significantly since the mid-1970s, with mean annual concentrations increasing over 50%. While previous work had suggested that nutrients were at saturation levels for phytoplankton in the Delta (Jassby et al. 2002), more recent work has found that N forms and concentrations as well as N ratios to other nutrients may play an important role in phytoplankton ecology and uptake kinetics (Dugdale et al. 2015; Glibert et al. 2016). These complex relationships between nutrients and Delta ecology highlight the importance of adequately characterizing and accounting for all internal and external nutrient sources in this system.

Dominant N sources to the Delta at present include upstream rivers and wastewater treatment plants. The Sacramento River and the San Joaquin River generally represent about 84% and 13% of water inflow to the Delta, respectively (Jassby and Cloern 2000). Together, they deliver over 17 million kg of total N (TN), as particulate and dissolved inorganic and organic N annually (Jassby and Cloern 2000; Saleh and Domagalski 2015). Diffuse (non-point source) agricultural sources upstream of the Delta account for the majority of TN in these rivers (Saleh and Domagalski 2015). A major anthropogenic point source of TN to the Delta is the Sacramento Regional Wastewater Treatment Facility (SRWTP), which underwent upgrades from advanced secondary treatment to tertiary treatment with biological nutrient removal that were close to

completion in April 2021. Before the upgrade, SRWTP annually discharged around 4 million kg of TN into the Sacramento River in the northern portion of the Delta, and the SRWTP TN input comprised roughly 32% of the Sacramento River annual TN load, though the importance of the SRWTP TN load was amplified during low flow months when contributions from other sources decreased (Saleh and Domagalski 2015). The SRWTP TN input predominantly occurred as NH_4^+ , and SRWTP NH_4^+ inputs were thought to account for over 90% of NH_4^+ input into the Sacramento River (Jassby 2008). Post-upgrade, SRWTP NH_4^+ concentrations in the discharged effluent have decreased to near zero, and TDN concentrations have declined by roughly 60% to 70% (<https://ciwqs.waterboards.ca.gov/>). This decrease has substantially lowered N inputs from SRWTP. With this reduction, NH_4^+ and TDN contributions from other sources, such as drainage from subsided islands in the central Delta, may increase in relative importance as sources of N to Delta waterways.

The Delta contains over fifty peat islands, many of which are artificially drained and commercially farmed. Long-term drainage of Delta islands for farming has resulted in extensive land subsidence from soil oxidation, with many islands now residing more than 3 m below sea level (Deverel and Leighton 2010). As a result, most Delta islands must artificially maintain water tables below the land surface via managed pumping. Water pumped off Delta islands is commonly referred to as agricultural drainage, return flow, and/or island drainage, and here we use “island drainage” to refer to this flow. Previous estimates of water discharge from island drainage ($\sim 1.5 \times 10^6 \text{ m}^3\text{d}^{-1}$) are comparable in magnitude to those from major wastewater treatment plants, such as SRWTP ($\sim 5.5 \times 10^5 \text{ m}^3\text{d}^{-1}$) (Templin and Cherry 1997). However, nutrient budgets for the Delta generally only account for upstream river and wastewater inputs, and Delta island drainage inputs remain elusive since they are widely under-studied. There may be over 200 active island drainage outfalls in the Delta; however, even our knowledge of drain locations is outdated (Siegfried et al. 2014).

Recent companion work by Richardson et al. (2020) found that island drainage is an important seasonal source of carbon to the Delta, and also showed that seasonal increases in dissolved carbon concentrations in island drainage are best explained by water table rises that help mobilize carbon in island soils. This seasonality in carbon cycling and transport raises important questions regarding concomitant changes in N species and other nutrient and trace element concentrations in drainage waters. Fluctuations in water table elevation and flow can shift the oxic-anoxic boundary in the subsurface, with subsequent effects on biogeochemical processes that ultimately control island drainage water quality. Microbial processing of carbon in the saturated zone is largely controlled by the influx of oxygenated waters, water residence times, nutrient availability, and the availability of carbon for respiration (Limpens et al. 2008). When O_2 demand is greater than O_2 influx, anoxic conditions can develop given sufficient carbon substrate. Naturally reduced zones (NRZs) exist in these saturated areas where organic matter is abundant and oxidant-consuming reactions are continuous (Yabusaki et al. 2017). As a result, NRZs can affect concentrations of dissolved organic carbon (DOC), dissolved inorganic N (DIN), dissolved organic N (DON), and reduced metal species (Du Laing et al. 2009; Yabusaki et al. 2017). Past work has shown that both trace elements and organo-metal complexes, like methylmercury, can be mobilized in Delta soils (Alpers et al. 2014; Bachand et al. 2019; Stumpner et al. 2015). As such, island drainage in the Delta may contribute seasonally important fluxes of both oxidized and reduced N species as well as other macronutrients and trace elements mobilized in wet-dry cycled NRZs.

To address this gap in knowledge, we measured monthly island drainage nutrient (NH_4^+ , NO_3^- , NO_2^- , PO_4^{3-} , DON, PON, SiO_4^{4-}) and trace element (total dissolved Fe, Mn, As) concentrations along with discharge on Sherman, Staten, and Twitchell islands in the Delta from June 2017 to September 2018 (Figure 1). Island drainage discharge volumes were used together with constituent concentrations to calculate island-

level gross fluxes. Inflow water volumes, taken as the collective sum of seepage and diversions, to Delta islands were calculated using a water budget approach, and river nutrient and trace element concentrations were used with the calculated water inflow volumes to estimate inflow gross fluxes. Island drainage net fluxes were subsequently calculated by subtracting the drainage fluxes (off-island) from the river inflow fluxes (on-island). We then upscaled island-level fluxes to the entire Delta to establish baseline estimates of (1) the timing and magnitude of this poorly characterized input to the larger Delta environment and (2) the regional importance of island drainage in the context of other major freshwater inputs under pre- and post-SRWTP upgrade conditions.

METHODS

Site Description

Drainage from three Delta islands was sampled in this study: Sherman (SH), Staten (ST), and Twitchell (TW) islands (Figure 1A through 1D). Island drainage from each of these Delta islands is discharged via outfalls that connect island pump stations to Delta channels. Sherman Island has five pump stations and is dominated by pastureland (67%) and cropland (30%) (Table A1). Staten Island has two pump stations and is predominantly cropland (93%). Twitchell Island has one pump station and is mixed land use made up approximately of cropland (48%), pastureland (22%), and several managed wetlands (30%). These islands are surrounded by river channels and sloughs from which water is siphoned or pumped for irrigation, a practice commonly referred to as diversion. These channels are also a source of seepage waters onto the islands. To characterize nutrient and element inputs onto the islands, surrounding river channels were also sampled.

Water Analyses

Water samples were collected monthly from all drains on the three islands as well as from seven surrounding river channels from June 2017 through September 2018 for nutrients (NH_4^+ , NO_3^- , NO_2^- , DON, PO_4^{3-} , SiO_4^{4-}), carbon species

(DOC, DIC), stable isotopes of nitrate ($\delta^{15}\text{N}\text{-NO}_3^-$ and $\delta^{18}\text{O}\text{-NO}_3^-$), and select trace elements (total dissolved As, Mn, Fe) (Figure 1). Samples for total suspended solids (TSS), $\delta^{15}\text{N}\text{-NH}_4^+$, $\delta^{15}\text{N}\text{-PON}$, and $\delta^{15}\text{N}\text{-DON}$ were collected quarterly during the same sampling events. A multi-parameter water-quality meter (YSI Pro Plus) was used to measure ancillary water parameters (pH, dissolved oxygen, conductivity, and temperature) at the time of sample collection. We do not report data for sites where monthly discharge was zero during the study period (e.g., May 2018 to September 2018 at SH-P4 and all of SH-P1). Similarly, all carbon data are presented separately in the Richardson et al. (2020) companion paper.

Water samples for all analyses, except trace elements, were vacuum filtered in the lab to 0.7 μm (pre-combusted Whatman GF/F) first and then 0.2 μm (Millipore Nylon Membrane). Water samples for trace elements were filtered on-site to 0.45 μm using trace-clean certified capsule filters (Geotech) and immediately acidified to pH < 2 with triple-distilled trace clean HCl. Samples were kept on ice until filtered and subsequently frozen or refrigerated, as dictated by their storage requirements.

All nutrient and trace element concentrations were determined at the Marine Analytical Laboratory at the University of California at Santa Cruz. Nutrients were measured on a Lachat QuikChem 8000 Flow Injection Analyzer. DON was determined indirectly by conversion to inorganic N using Kjeldahl digestions and run on a Lachat QuikChem 8000 Flow Injection Analyzer. Dissolved trace element concentrations were determined on a Thermo ElementXR High-Resolution Inductively Coupled Plasma Mass Spectrometer and run together with certified reference materials (NIST Standard Reference Material 1643f). DOC concentrations were measured as non-purgeable organic carbon (NPOC) on a Shimadzu TOC-VCPH TOC/TN Analyzer. Island drainage particulate organic matter (POM) concentrations were estimated from TSS concentrations as described in Richardson et al. (2020), and molar ratios of C to N (C:N_m) of POM values were used to

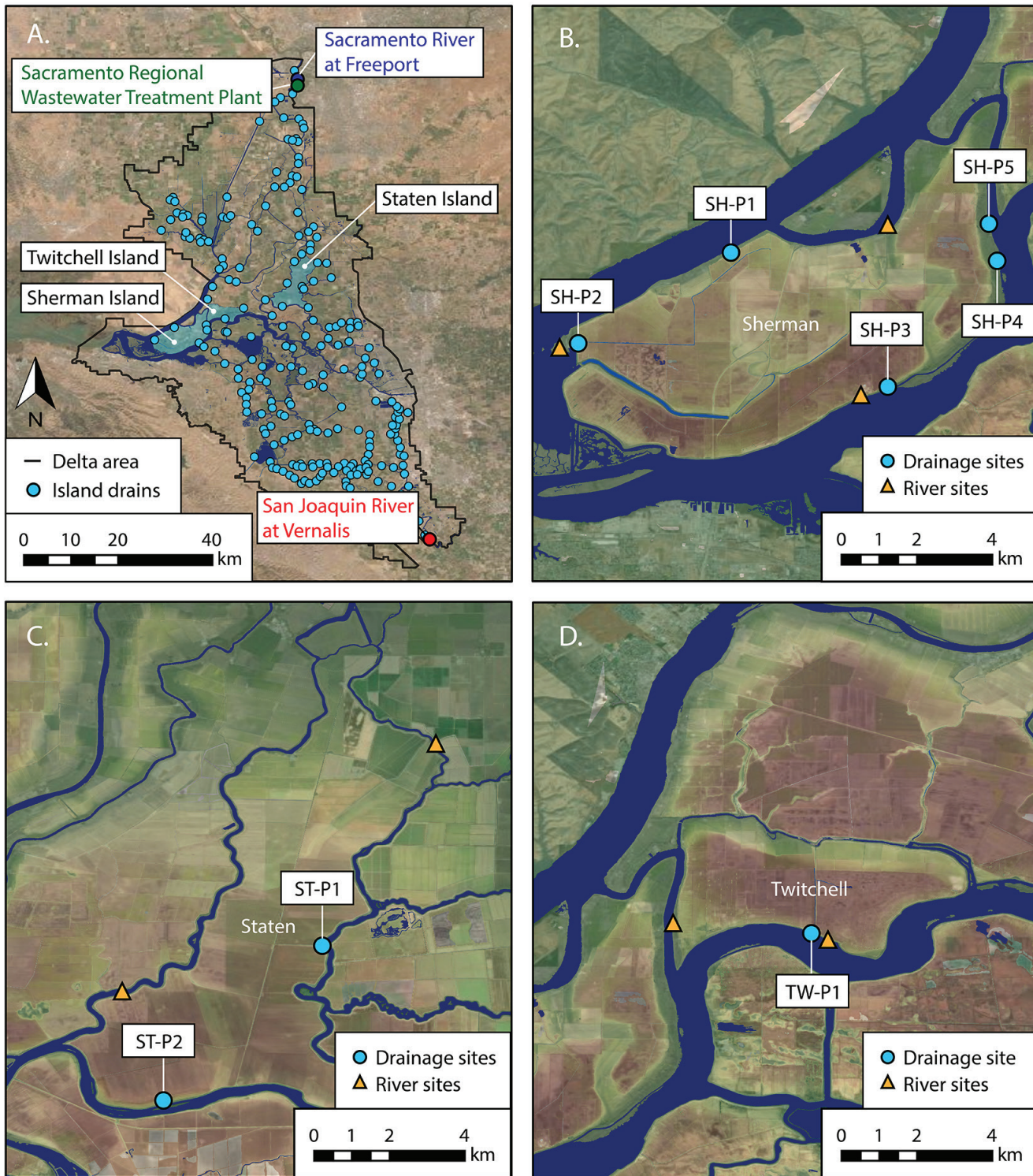


Figure 1 (A) Overview of the Sacramento–San Joaquin Delta showing the location of, the Sacramento River at Freeport, Sacramento Regional Wastewater Treatment Plant, San Joaquin River at Vernalis, and the three islands sampled in this study. Island drain locations for the entire Delta are shown as *blue circles* based on a digitized map from CDWR (1995). (B–D) Maps of Sherman, Staten and Twitchell Island indicating locations of island drain (*blue circles*) and river (*orange triangles*) sites sampled on each island. All study area maps are oriented such that North is up. Site abbreviations are as follows: Sherman Island (SH), Staten Island (ST), and Twitchell Island (TW).

estimate PON concentrations. For river samples, we used the previously published relationship between TSS and POC for the Delta's rivers from Murrell and Hollibaugh (2000) to calculate POC concentrations, and then used $(C:N)_m$ ratios to generate PON concentrations. This method assumes around 5% of riverine TSS is POC, which is in line with more recent work by Hernes et al. (2020). Precision and accuracy were below 5% for all nutrients and below 8% for trace elements. Annual means and standard deviation of geochemical data are presented for the 2018 water year (October 2017 to September 2018), a below-normal water year which we refer to herein as "dry."

Stable isotope samples ($\delta^{15}\text{N-NH}_4^+$, $\delta^{15}\text{N-NO}_3^-$, $\delta^{18}\text{O-NO}_3^-$, $\delta^{15}\text{N-PON}$, and $\delta^{15}\text{N-DON}$) were run at the USGS Menlo Park Stable Isotope Facility using the methods described in Kendall et al. (2015). All values are presented in permil notation (‰) relative to Vienna Air (VAIR) for $\delta^{15}\text{N}$ and Vienna Standard Mean Oceanic Water (VSMOW) for $\delta^{18}\text{O}$. Analytical precision for $\delta^{15}\text{N-NH}_4^+$, $\delta^{15}\text{N-NO}_3^-$, and $\delta^{18}\text{O-NO}_3^-$ was 1.1‰, 0.3‰, and 0.7‰, respectively. Analytical precision for $\delta^{15}\text{N-DON}$ and PON was 0.4‰.

Statistical analysis was performed in two steps: (1) a Kruskal-Wallis One Way Analysis of Variance on Ranks was completed to determine if seasonal values were statistically significantly different and (2) a coupled pairwise multiple comparisons procedure was then conducted using Dunn's Method to determine which seasonal values were different from one another. *P* values less than 0.05 were considered as significant for all statistical tests.

Discharge and Mass Flux Estimates

Water discharge from islands was measured as discussed by Richardson et al. (2020). Briefly, records documenting electrical usage, *P* (kW-hr), from each pump station were used together with pump efficiency, *U* (kW-hr m⁻³), to calculate discharge, *D* (m⁻³), using the unit-power consumption method where $D = P/U$ (Ogilbee 1966; Ogilbee and Mitten 1970; Diamond and Williamson 1983). Discharge estimates from

TW-P1 on Twitchell Island were cross-checked with 1.5 years of daily flow meter data (AgriFlo XCi ultrasonic sensor) collected across the 2017 and 2018 water years. This cross-comparison indicated that the unit-power consumption method is a relatively robust approximation of discharge (slope = 0.87, $R^2 = 0.75$) that slightly underestimates actual discharge. As such, mass fluxes generated using these discharge estimates herein are considered conservative estimates (e.g., actual fluxes are likely higher).

Island drainage fluxes (mass per unit of time) or loads (mass) off-island into Delta waterways are referred to herein as gross fluxes or gross loads. Island drainage gross fluxes were calculated from monthly measured concentrations and discharge data for each drainage site. For islands with more than one drain (Sherman and Staten islands), monthly loads were summed from all drainage sites. All fluxes in this study are reported as elemental mass per unit of time. PON fluxes were calculated quarterly, at the same frequency as sample collection, and these fluxes were assumed to represent their respective seasonal contributions. Seasons were defined as follows: fall (September through November), winter (December through February), spring (March through May), and summer (June through August).

Island drainage gross mass fluxes were upscaled to Delta-wide contributions using seasonal mean geochemistry data from this study and an annual volumetric estimate of drainage discharge, $\sim 5.3 \times 10^8 \text{ m}^3$, from Templin and Cherry (1997). First, to calculate monthly regional drainage volumes, the annual discharge volume was scaled to monthly time-steps using monthly flow percentages calculated from discharge data in this study, where discharge for each month was calculated as a percentage of total water year discharge (Table A2). Flow percentages were generated for Sherman Island, a pastureland-dominated land use, and Staten Island, a cropland-dominated land use. This assumes that the hydrologic regime of each island is, generally, regionally representative of these two land-use groups. Monthly discharge values for these

two land-use types in the Delta were summed to seasonal scales and then used together with seasonal mean concentration data for each island in subsequent gross and net flux calculations. The seasonal mean concentration data were not averaged equally across these islands, which have multiple drainage outlets; instead, we divided the island-scaled seasonal gross loads by their seasonal outflow volumes to obtain a spatially integrated mean concentration. This method gives greater weight to stations that have higher discharge rather than averaging across stations that may not discharge as much as nearby sites. The gross flux calculations resulted in two unique estimates: (1) upscaled gross mass fluxes based on Staten Island (cropland) flow percentages and geochemistry, and (2) upscaled gross mass fluxes based on Sherman Island (pastureland) flow percentages and geochemistry. Twitchell Island data were not used for upscaling because of its mixed land use. Around 82% of the region within the legal boundary of the Delta is cropland and 18% is pastureland, idle, or grassland (based on spatial data available online from the California Crop Mapping database <https://data.cnra.ca.gov/dataset/statewide-crop-mapping>). These spatial coverage percentages were used to weight the previously discussed upscaled fluxes based on dominant land use in the Delta, and the data presented herein are the spatially weighted averages of these two estimates. Upscaled net flux estimates are discussed below.

Inflow Water Flux Estimates

To calculate net fluxes for Delta islands, we used a water budget approach to first estimate annual and seasonal water inflow to each island as follows:

$$I = O + ET - P$$

where I is total inflow (or import), including groundwater infiltration and diversions that bring river water onto the island (m^3), O is outflow (or export) from island drainage pumps (m^3), ET is evapotranspiration (m^3), and P is precipitation (m^3). Water budget data are provided in Appendix A, Tables A3 (annual) and A4 (seasonal). P was based on measured data

from Station 247 for Sherman Island, Station 242 for Staten Island, and Station 140 for Twitchell Island via California Irrigation Management Information System (CIMIS; <https://cimis.water.ca.gov/>). ET was calculated at a monthly scale and summed to seasonal and annual scales by correcting monthly reference ET rates using crop coefficients for land use cover on each island for the dry 2018 water year (<http://www.itrc.org/etdata/index.html>). Our seasonal ET and P estimates at the island level were in close agreement with values estimated by the Delta Channel Depletion (DCD) model ($R^2 = 0.98$ for ET and $R^2 = 0.92$ for P ; 2020 email between L Liang and CM Richardson, unreferenced, see “Notes”). Change in storage was assumed to be negligible on an annual scale, based on previous studies that show island water tables are generally stable at this time-scale (Deverel et al. 2015; Deverel et al. 2016). Since our outflow values were measured directly, the close alignment of ET and P estimates with DCD suggests that our island-level inflow estimates are relatively robust at the annual scale. Our island-level outflow values did differ substantially and non-linearly from DCD estimates though, with seasonal comparisons of measured outflow from this study vs. DCD estimates poorly correlated ($R^2 = 0.02$).

To estimate mass fluxes at greater temporal resolution than yearly, we also assumed that change in water storage was negligible seasonally across the 2018 water year. We recognize that this assumption probably does not reflect actual seasonal changes in water storage on Delta islands. The consequence of this assumption is that our seasonal water budgets may be overestimating water inflow when on-island water storage decreases (likely in the spring/summer) and underestimating water inflow when on-island water storage increases (likely in the fall/winter). However, the use of these seasonal water inflow volumes is roughly supported by inflow values estimated by the DCD model, which were generally the same order of magnitude and positively correlated to one another ($R^2 = 0.88$, slope = 0.96). As such, we believe our seasonal net fluxes, made possible by the seasonal water budgets, provide useful new insights that

warrant discussion herein. At the same time, we also recognize that there is uncertainty in the estimated seasonal water inflow volumes. This uncertainty could be better assessed with island groundwater level data, which are generally not currently available.

To estimate Delta-wide inflow, we used the above island-level inflow data and calculated seasonal inflow-to-outflow ratios for pastureland-dominated islands (Sherman Island) vs. cropland-dominated islands (Staten Island). These were used to scale previously reported Delta-wide island drainage water outflow ($\sim 5.3 \times 10^8 \text{ m}^3$) from Templin and Cherry (1997) to inflow (Table A4). Our annualized Delta-wide inflow-to-outflow ratio generally agreed with the value estimated by the DCD model, though volumetric magnitudes differed, with the DCD model estimating about two times the outflow volume we use herein for regional upscaling from Templin and Cherry (1997). The volumetric difference between the two methods suggests that our results can be considered conservative estimates that likely under-value the contribution of these waters.

Net Mass Flux Estimates

River nutrient and trace element concentrations were averaged seasonally from monthly samples for (1) only the river sites that surround each island, to calculate island-level inflow mass flux estimates, and (2) all river sites, to calculate river inflow mass fluxes at the Delta-wide scale (Table A5). The island-level and Delta-wide inflow water volumes, used to calculate inflow mass fluxes, were taken directly from water budget calculations as discussed above. The inflow mass fluxes were then subtracted from gross outflow fluxes at the island and Delta-wide level to calculate net mass fluxes.

Pre- and Post-Upgrade Comparison of Wastewater, Island Drainage, and River Mass Fluxes

Monthly concentration (dissolved N and P) and discharge data were aggregated from the Sacramento River at Freeport (USGS 11447650), San Joaquin River at Vernalis (USGS 11303500), and SRWTP for seasonal mass flux comparisons to our Delta-wide island drainage net fluxes

for water year (WY) 2018 (USGS 2019). The Sacramento River at Freeport site is located just upstream of the SRWTP discharge point. Concentration and flow data for SRWTP fluxes for WY 2018 were downloaded via the California Integrated Water Quality System and used in pre-upgrade SRWTP flux calculations (<https://www.waterboards.ca.gov/ciwqs/>). Additionally, SRWTP only had data released for TP for the first 3 months of WY 2018, while all other N species had data availability for the full water year; our TP estimates for WY 2018 are thus based on these 3 months. Predicted post-upgrade dissolved N (TDN = $528 \mu\text{M}$, NH_4^+ = $11.4 \mu\text{M}$, NO_3^- = $480 \mu\text{M}$) and P concentrations (TP = $73 \mu\text{M}$, unchanged) in SRWTP effluent were used together with WY 2018 discharge volumes to estimate post-upgrade SRWTP mass fluxes (LWA 2014). We assume reported SRWTP TP concentrations are roughly equivalent to PO_4^{3-} as PO_4^{3-} is the dominant component of TP in SRWTP effluent.

RESULTS

Island Drainage Discharge and Water Quality

Island drainage discharge was highly variable across sites and water years, though seasonal trends were apparent (Figure 2). Discharge was generally greatest in the winter across all three islands, with 49 ± 6 and $32 \pm 10\%$ of annual discharge occurring in winter of WY 2017 and 2018, respectively (Table A2). Cumulative discharge was 1.2 to 2.2 times greater in wet WY 2017 than dry WY 2018 across all islands.

Monthly averaged island drainage nutrient and trace element concentrations showed seasonal trends for many, though not all, constituents (Figure 3). TDN, DON, NH_4^+ , SiO_4^{4-} , and total dissolved Mn were significantly higher in the winter and spring across all sites compared to the summer ($p < 0.05$), while NO_3^- and NO_2^- concentrations were more variable, but generally higher in the winter and spring. Island drainage TDN concentrations averaged $201 \pm 104 \mu\text{M}$ (defined as the mean \pm one standard deviation) in fall, $240 \pm 109 \mu\text{M}$ in winter, $199 \pm 60 \mu\text{M}$ in spring, and $93 \pm 22 \mu\text{M}$ in summer. A majority of TDN was comprised of DON, and DON concentrations were

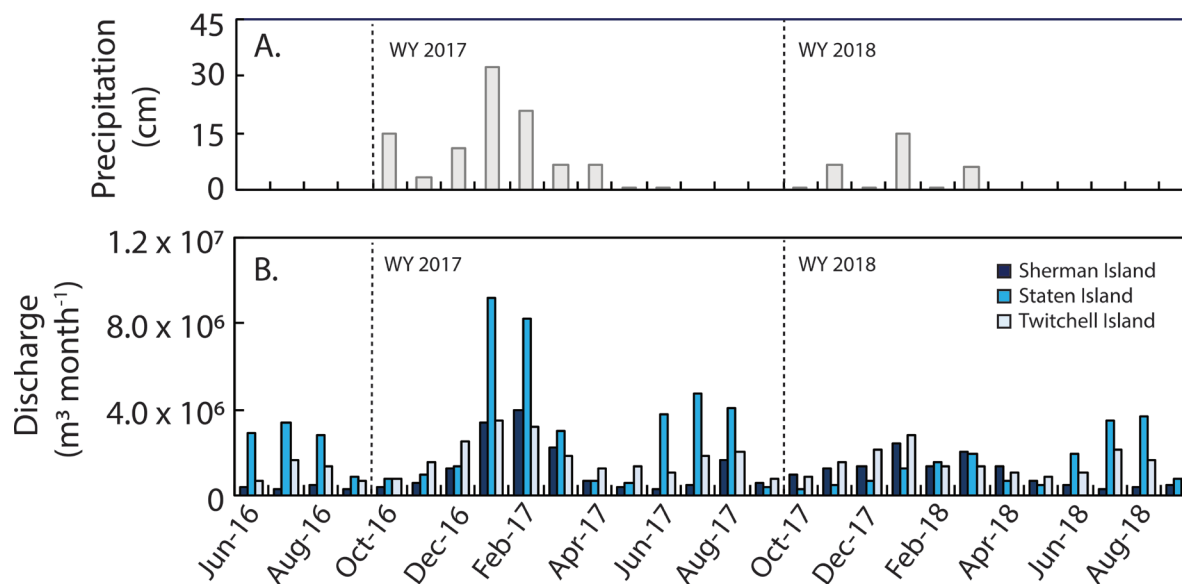


Figure 2 (A) Monthly precipitation and (B) discharge from Sherman, Staten, and Twitchell Islands. Precipitation data were acquired from Station 242 via the California Irrigation Management Information System (CIMIS). Discharge data were determined using the unit-power consumption method and cross-checked with measured flow meter estimates discussed in Methods.

statistically significantly different across seasons at 161 ± 99 , 132 ± 56 , 115 ± 42 , and $79 \pm 39 \mu\text{M}$, in fall, winter, spring, and summer, respectively ($p < 0.05$). Relative proportions of DIN and DON shifted seasonally as well, with DIN generally increasing in relative proportion during winter and spring compared to summer and fall. NH_4^+ concentrations were typically higher than NO_3^- and thus comprised a larger proportion of DIN in island drainage, except for some dates on Staten Island where NO_3^- concentrations were elevated. NH_4^+ concentrations averaged $14 \pm 11 \mu\text{M}$ across all sites in summer months and were notably higher at $26 \pm 17 \mu\text{M}$ in fall, $61 \pm 35 \mu\text{M}$ in winter, and $60 \pm 44 \mu\text{M}$ in spring, respectively ($p < 0.05$). NO_3^- concentrations in island drainage averaged $10 \pm 10 \mu\text{M}$ across all sites in summer months, and were significantly higher in winter ($34 \pm 58 \mu\text{M}$) ($p < 0.05$), while fall and spring had mean concentrations of $15 \pm 34 \mu\text{M}$ in fall and $23 \pm 35 \mu\text{M}$ in spring, respectively. Island drainage PON concentrations did not show a consistent seasonal pattern and averaged $210 \pm 70 \mu\text{M}$ in fall, $120 \pm 61 \mu\text{M}$ in winter, $156 \pm 74 \mu\text{M}$ in spring, and $180 \pm 58 \mu\text{M}$ in summer. PO_4^{3-} concentrations in drainage were variable across sites and through

time as well, with concentrations only slightly higher in summer months ($2.7 \pm 1.2 \mu\text{M}$) relative to winter ($1.6 \pm 0.8 \mu\text{M}$). Concentrations of SiO_4^{4-} in island drainage were significantly lower in the summer ($380 \pm 130 \mu\text{M}$) relative to fall, winter, and spring, when means ranged between $540 \pm 160 \mu\text{M}$ to $600 \pm 140 \mu\text{M}$ ($p < 0.05$). Total dissolved Mn concentrations were significantly higher during fall ($670 \pm 210 \mu\text{g L}^{-1}$), winter ($760 \pm 370 \mu\text{g L}^{-1}$), and spring ($1100 \pm 740 \mu\text{g L}^{-1}$) compared to summer ($310 \pm 300 \mu\text{g L}^{-1}$) as well ($p < 0.05$). Total dissolved Fe and As concentrations showed no significant seasonal trends, with means ranging between 820 ± 970 to $1550 \pm 1450 \mu\text{g L}^{-1}$ for Fe and $5.5 \pm 5.0 \mu\text{g L}^{-1}$ for As across all seasons.

At an annual scale, mean island drainage TDN, NH_4^+ , NO_2^- , DON, PON, and SiO_4^{4-} concentrations for WY 2018 were always greater than surrounding rivers at all sites, while NO_3^- and PO_4^{3-} concentrations were more variable, with concentrations both higher and lower than nearby rivers (Table 1). Mean annual dissolved Mn, Fe, and As concentrations were generally higher in island drainage, by up to two orders of magnitude, relative to river water (Table 1).

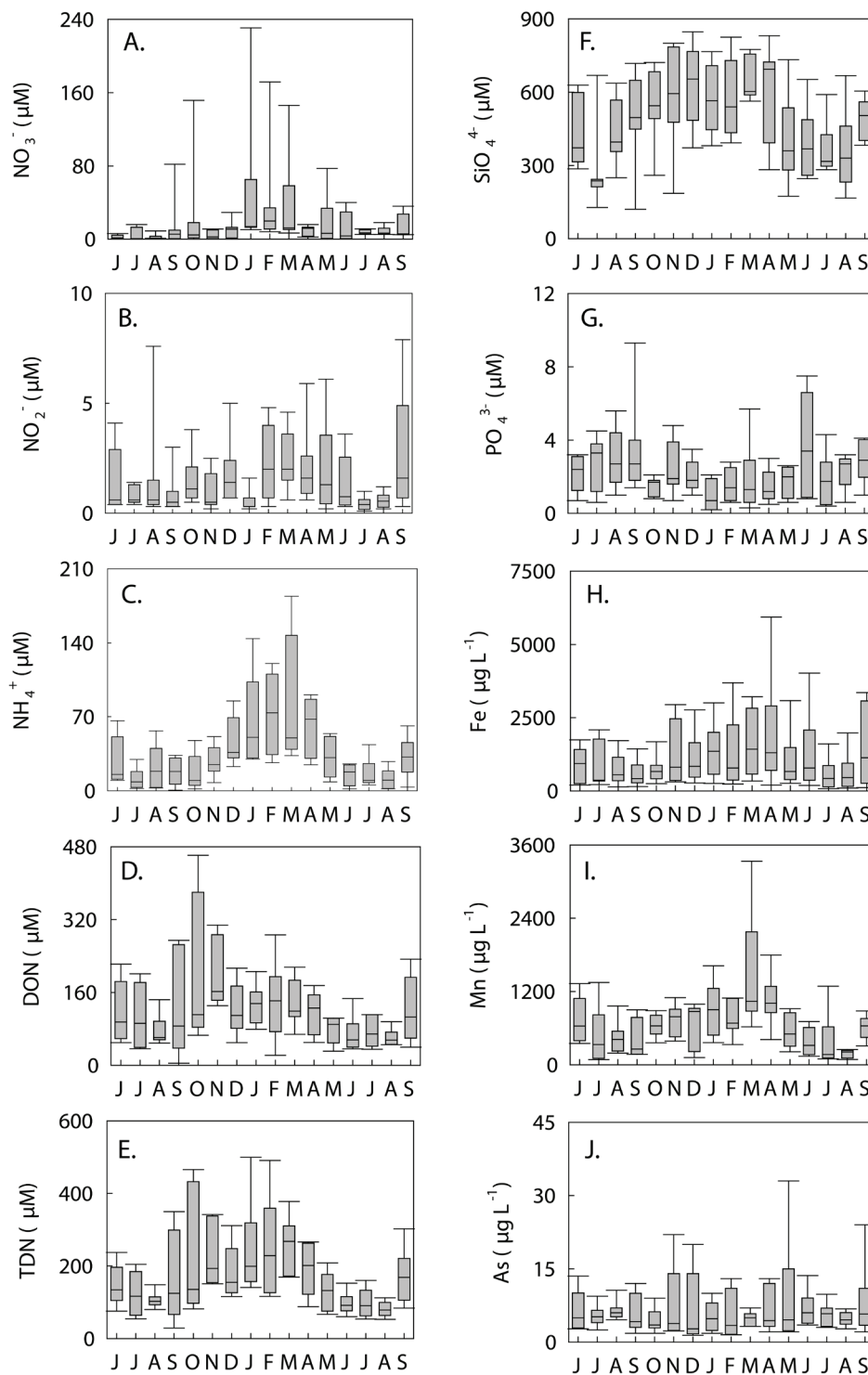


Figure 3 Box plots of monthly island drainage concentrations from all sites, starting in June 2017 through September 2018, for (A) NO_3^- , (B) NO_2^- , (C) NH_4^+ , (D) dissolved organic N (DON), (E) total dissolved N (TDN), (F) SiO_4^{4-} , (G) PO_4^{3-} , (H) total dissolved Fe, (I) total dissolved Mn, and (J) total dissolved As. Boxes represent the bounds of the middle quartiles, and lines represent median values. Whiskers show the bounds of the outer quartiles (5th and 95th) of the data.

Table 1 Mean and standard deviation of river and island drainage geochemistry collected monthly during water year (WY) 2018 between October 2017 and September 2018. WY 2017 data are not included so as not to bias the annual mean.

		Rivers	SH-P2	SH-P3	SH-P4 ^a	SH-P5	ST-P1	ST-P2	TW-P1
TN (μM)	mean	65	386	468	230	328	352	370	227
	stdev	46	74	98	115	62	114	134	12
TDN (μM)	mean	56	183	272	168	113	188	262	126
	stdev	25	87	136	52	44	105	155	45
$\text{NO}_3^- + \text{NO}_2^-$ (μM)	mean	22	10	24	12	12	49	35	10
	stdev	11	12	48	9	5	55	65	8
NH_4^+ (μM)	mean	6	53	56	39	24	29	48	36
	stdev	5	56	58	19	13	20	23	20
DON (μM)	mean	29	119	192	113	75	107	174	80
	stdev	27	35	105	48	32	67	109	39
PON (μM)	mean	8	218	210	53	204	175	129	105
	stdev	7	28	28	28	48	86	53	51
SiO_4^{4-} (μM)	mean	250	310	440	790	670	510	540	500
	stdev	60	120	100	60	130	140	180	110
PO_4^{3-} (μM)	mean	1.7	1.0	1.8	2.5	2.4	2.2	1.6	3.1
	stdev	0.6	0.8	1.3	1.6	0.8	2.0	1.2	1.3
As ($\mu\text{g L}^{-1}$)	mean	1.6	3.1	6.1	3.8	2.4	8.5	13.5	4.8
	stdev	0.5	1.2	3.0	3.3	0.8	3.3	9.2	1.4
Mn ($\mu\text{g L}^{-1}$)	mean	30	1120	860	780	620	640	600	430
	stdev	30	820	550	710	250	350	380	180
Fe ($\mu\text{g L}^{-1}$)	mean	60	820	310	1820	1030	1020	1650	2020
	stdev	60	830	200	2070	740	770	1230	1000
$\delta^{15}\text{N-PON}$ (‰)	mean	4.9	3.0	3.3	0.1	-0.1	3.2	2.4	1.6
	stdev	2.1	3.4	3.2	3.0	0.5	0.9	1.5	1.4
$\delta^{15}\text{N-DON}$ (‰)	mean	1.8	0.1	1.8	0.9	0.3	1.7	1.6	1.8
	stdev	2.1	2.1	2.3	0.4	1.0	0.7	0.5	1.7
$\delta^{15}\text{N-NH}_4^+$ (‰)	mean	9.9	9.0	9.8	9.3	9.0	11.9	11.2	10.3
	stdev	5.6	4.3	2.3	1.4	1.8	1.7	2.3	2.4
$\delta^{15}\text{N-NO}_3^-$ (‰)	mean	7.0	4.7	3.5	5.2	4.0	12.8	15.2	3.8
	stdev	1.4	3.4	2.3	7.5	1.7	6.6	6.7	3.9

a. SH-P4 water year data are incomplete as data collected during net zero discharge months were not included.

$\delta^{15}\text{N}$ values of PON, DON, NH_4^+ , and NO_3^- indicated clear differences in stable isotope composition amongst N pools that were common to all island drainage sites (Figure 4A). DON and PON pools overlapped in concentration range and N stable isotope composition, ranging from 120 to 150 μM and $1.2 \pm 0.5\text{‰}$ to $2.2 \pm 1.6\text{‰}$, on average, respectively. Concentrations of NH_4^+ were similar or lower than organic N pools and generally had

higher $\delta^{15}\text{N}$ values, around $10.3 \pm 1.1\text{‰}$ on average, compared to PON and DON. Concentrations of NO_3^- and $\delta^{15}\text{N-NO}_3^-$ values were generally lower and more variable than the NH_4^+ pool, with mean $\delta^{15}\text{N-NO}_3^-$ values of $6.7 \pm 3.2\text{‰}$.

Island Drainage Nutrient and Trace Element Fluxes

Island-level gross TN and TDN fluxes, calculated from monthly concentration and discharge data,

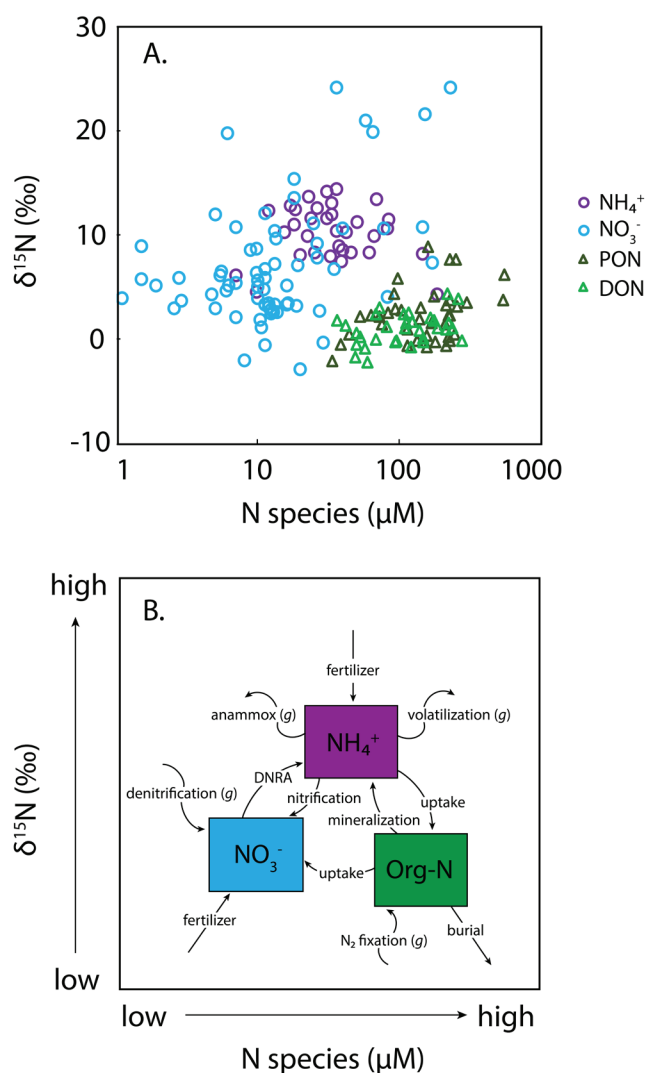


Figure 4 (A) $\delta^{15}\text{N}$ values versus N species concentration for NH_4^+ (purple), NO_3^- (blue), particulate organic N (PON) (dark green), and dissolved organic N (DON) (light green). Circular markers represent inorganic N pools and triangular markers represent organic N pools. (B) Conceptual model of the relative relationship between $\delta^{15}\text{N}$ values and concentration for major dissolved and particulate N pools on Delta islands. Model shows interconnecting processes, but arrows are qualitative and do not refer to the direction of concentration or $\delta^{15}\text{N}$ change. DNRA represents dissimilatory nitrate reduction to ammonium. Double curved arrows represent conversions to or from various gaseous (g) N forms.

ranged from 70 to 230 kg d^{-1} and 20 to 100 kg d^{-1} in the summer and 170 to 320 kg d^{-1} and 120 to 200 kg d^{-1} in the winter, respectively (Table 2, Figure 5). Organic N accounted for ~79 to 81% of gross annual TN fluxes across all sites (with 40% to 48% and 29% to 39% of the gross TN flux as PON and DON, respectively), while DIN accounted for the remaining ~19% to 21%. Island drainage gross SiO_4^{4-} fluxes peaked in the winter (610 to 820 kg d^{-1}), while gross PO_4^{3-} fluxes were generally greatest during the summer (1 to 7 kg d^{-1}). Island drainage gross total dissolved Mn and Fe fluxes ranged between 10 and 70 kg d^{-1} and 10 to 110 kg d^{-1} , respectively, and were seasonally greatest in the winter on all islands (Table 2). Island drainage gross total dissolved As fluxes ranged between 0.1 to 0.5 kg d^{-1} across all sites and seasons. While nutrient and trace element gross fluxes generally peaked in the winter, Staten and Twitchell islands also experienced secondary peaks in mass fluxes during summer.

After accounting for inflow fluxes, island-level net drainage fluxes were highest in the winter and spring for all measured species (Table 2). Islands were generally net sinks in the summer for TDN (0 to -130 kg d^{-1}), $\text{NO}_3^- + \text{NO}_2^-$ (-20 to -50 kg d^{-1}), SiO_4^{4-} (-440 to -1310 kg d^{-1}), and PO_4^{3-} (-3 to -12 kg d^{-1}), and Sherman Island was a temporary sink for all DIN species and DON in the summer. Annual net island level fluxes were positive for both TDN and TN across all islands, though $\text{NO}_3^- + \text{NO}_2^-$ fluxes were net negative on both Sherman and Twitchell islands.

Upscaled to annual Delta-wide contributions, island drainage contributed an estimated total annual gross TN load of 2.7×10^6 kg to Delta waterways in WY 2018 (Table 3). Similar to island-level estimates, the annual gross TN load was compositionally dominated by PON (43%) and DON (34%), with DIN comprising the remaining 24% (see Figure 6 for seasonal percentages). The annual total island drainage gross SiO_4^{4-} load was estimated to be about 7.6×10^6 kg, while the PO_4^{3-} load was about 2.8×10^4 kg (Table 3). Annual gross total dissolved Mn and Fe loads from all islands were similar in magnitude, 3.7×10^5 to 5.9×10^5 kg, while total dissolved As contributions were

Table 2 Seasonal gross and net island drainage nutrient and trace element fluxes for each island for water year 2018 calculated by season (Fall: September to November; Winter: December to February; Spring: March to May; Summer: June to August), and for the water year (annual).

	Season	TN (kg d ⁻¹)	TDN (kg d ⁻¹)	NO ₃ ⁻ + NO ₂ ⁻ (kg d ⁻¹) ²	NH ₄ ⁺ (kg d ⁻¹)	DON (kg d ⁻¹)	PON (kg d ⁻¹)	SiO ₄ ⁴⁻ (kg d ⁻¹)	PO ₄ ³⁻ (kg d ⁻¹)	As (kg d ⁻¹)	Mn (kg d ⁻¹)	Fe (kg d ⁻¹)
Gross												
Sherman	Fall	140	90	0	10	80	50	370	2	0.1	20	20
	Winter	320	200	30	60	110	110	820	2	0.2	60	40
	Spring	340	150	10	50	80	190	660	2	0.2	70	50
	Summer	70	20	0	0	20	50	150	1	0.1	10	10
	Annual	220	110	10	30	70	100	500	2	0.1	40	30
Staten	Fall	150	60	10	10	50	80	260	2	0.2	10	20
	Winter	170	140	30	30	80	30	610	1	0.4	30	80
	Spring	250	110	40	30	40	140	550	1	0.3	30	20
	Summer	230	100	30	20	60	130	860	7	0.5	10	40
	Annual	200	100	30	20	60	100	570	3	0.4	20	40
Twitchell	Fall	110	70	0	10	50	40	460	4	0.2	20	70
	Winter	200	120	10	40	70	80	820	5	0.2	20	110
	Spring	90	60	10	20	40	20	570	3	0.1	20	50
	Summer	130	60	0	10	40	70	440	5	0.3	10	100
	Annual	130	80	10	20	50	50	570	4	0.2	20	80
Net												
Sherman	Fall	50	10	-30	0	0	40	-300	-4	0.0	20	20
	Winter	260	150	10	60	90	110	430	0	0.1	60	40
	Spring	190	10	-40	50	10	170	-230	-6	0.0	60	30
	Summer	-140	-130	-50	-10	-70	-20	-1170	-12	-0.4	-10	-10
	Annual	90	10	-30	20	10	80	-320	-6	-0.1	30	20
Staten	Fall	140	50	10	10	40	80	170	1	0.2	10	20
	Winter	160	140	30	30	80	30	580	1	0.4	30	80
	Spring	190	60	30	20	10	130	-20	-2	0.1	30	20
	Summer	50	-60	-40	-40	20	110	-1310	-8	-0.1	10	30
	Annual	140	50	10	0	40	90	-150	-2	0.2	20	40
Twitchell	Fall	70	20	-20	10	30	40	20	0	0.1	20	70
	Winter	130	60	-20	30	50	70	220	1	0.1	20	100
	Spring	20	0	-20	10	10	20	100	-2	0.0	20	50
	Summer	60	0	-20	10	10	60	-440	-3	0.0	10	100
	Annual	70	20	-20	20	30	50	-20	-1	0.0	20	80

the smallest of all loads and averaged around 4.4×10^3 kg annually.

Annual Delta-wide net island drainage fluxes were positive for all constituents measured except PO₄³⁻ (Table 3). Delta-wide net island drainage fluxes for TN and TDN averaged 5,030 kg d⁻¹ and 2,290 kg d⁻¹ annually, respectively. Delta-wide net

N fluxes totaled 570 kg d⁻¹ for NH₄⁺, 170 kg d⁻¹ for NO₃⁻ + NO₂⁻, 1,520 kg d⁻¹ for DON and 2,740 kg d⁻¹ for PON. Seasonally, Delta-wide island drainage fluxes were net negative in the summer for all constituents except for total dissolved Mn, suggesting that islands may act as temporary sinks for many constituents (Table 4). These upscaled net negative fluxes were overcome by

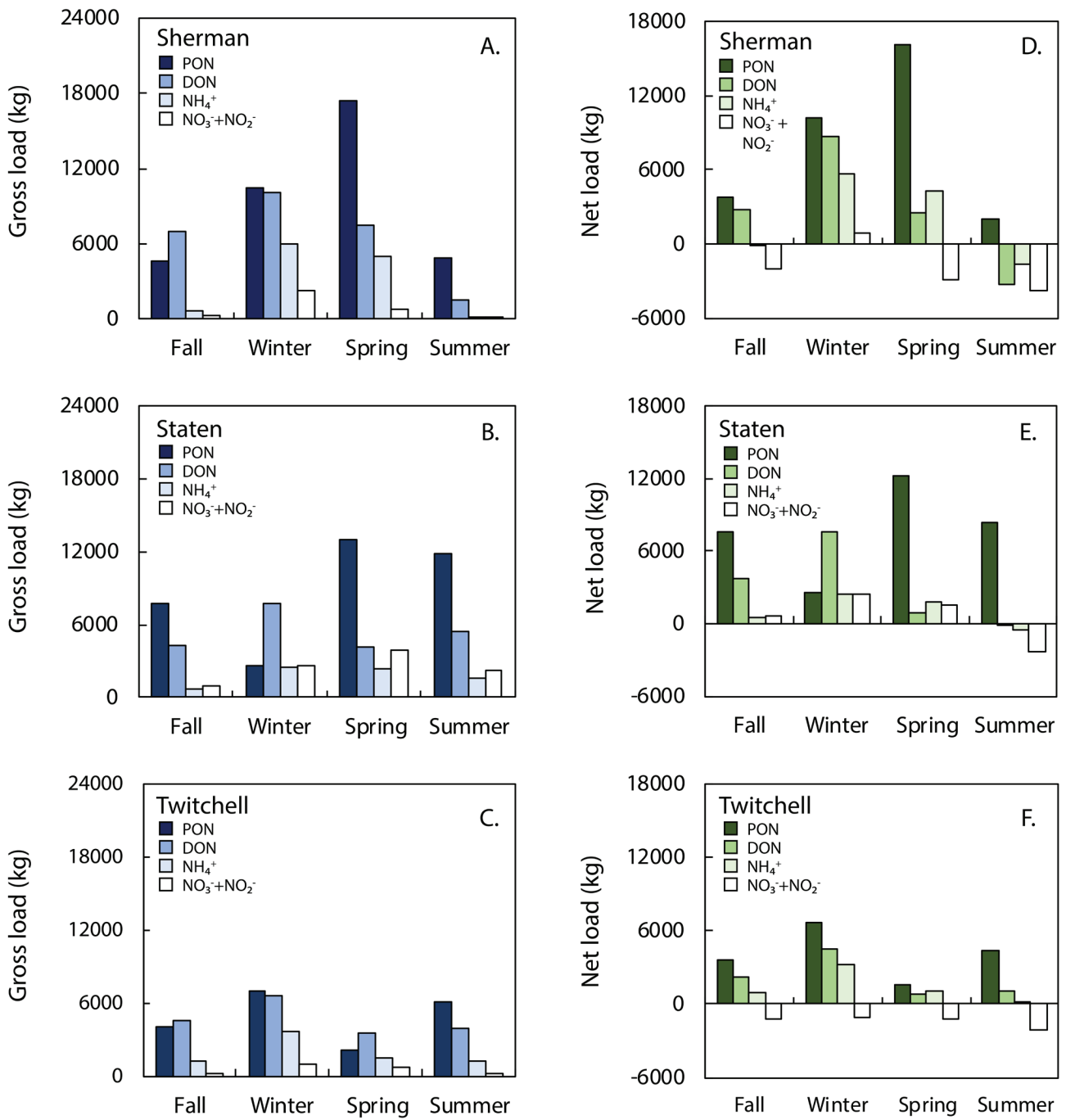


Figure 5 Seasonal (A-C) gross and (D-F) net island drainage nitrogen (N) species loads for (A, C) Sherman, (B, E) Staten, and (C, F) Twitchell Islands. Bar color refers to N species (NO₃⁻ + NO₂⁻, NH₄⁺, dissolved organic nitrogen (DON), particulate organic N (PON). See Table 2 for values.

Table 3 Upscaled Delta-wide island drainage gross fluxes, river inflow fluxes, and net fluxes for WY 2018 before any upgrades to the Sacramento Regional Wastewater Treatment Plant

	Annual island drainage load (kg)	Island drainage gross flux (kg d ⁻¹)	River inflow flux onto islands (kg d ⁻¹)	Mean annual net flux (kg d ⁻¹)	Annual net load (kg)
TN	2.7 x 10 ⁶	7,390	2,360	5,030	1.8 x 10 ⁶
TDN	1.5 x 10 ⁶	4,240	1,950	2,290	8.4 x 10 ⁵
NO₃⁻ + NO₂⁻	3.3 x 10 ⁵	910	750	170	6.2 x 10 ⁴
NH₄⁺	3.0 x 10 ⁵	830	260	570	2.1 x 10 ⁵
DON	9.1 x 10 ⁵	2,500	970	1,520	5.6 x 10 ⁵
PON	1.1 x 10 ⁶	3,150	410	2,740	1.0 x 10 ⁶
SiO₄⁴⁻	7.6 x 10 ⁶	20,770	19,270	1,490	5.4 x 10 ⁵
PO₄³⁻	2.8 x 10 ⁴	80	170	- 90	-3.3 x 10 ⁴
As	4.4 x 10 ³	10	10	10	2.3 x 10 ³
Mn	3.7 x 10 ⁵	1,010	80	930	3.4 x 10 ⁵
Fe	5.9 x 10 ⁵	1,620	180	1,440	5.3 x 10 ⁵

Table 4 Upscaled Delta-wide seasonal mean island drainage gross and net fluxes based on water year 2018 geochemistry data

	Fall (kg d ⁻¹)	Winter (kg d ⁻¹)	Spring (kg d ⁻¹)	Summer (kg d ⁻¹)
Gross				
TN	6,240	9,620	9,590	4,100
TDN	3,800	7,030	4,500	1,630
NO₃⁻ + NO₂⁻	520	1,500	1,270	380
NH₄⁺	360	1,500	1,190	270
DON	2,930	4,040	2,040	980
PON	2,440	2,590	5,100	2,470
SiO₄⁴⁻	14,930	31,890	22,750	13,500
PO₄³⁻	70	70	50	110
As	10	20	10	10
Mn	770	1,620	1,430	200
Fe	1,200	3,390	1,200	670
Net				
TN	5,470	9,150	6,910	- 1,410
TDN	3,120	6,600	2140	- 2,680
NO₃⁻ + NO₂⁻	250	1,330	320	- 1,220
NH₄⁺	280	1,460	1,000	- 470
DON	2,450	3,870	770	- 990
PON	2,350	2,560	4,780	1,270
SiO₄⁴⁻	8,470	28,540	4,560	- 35,600
PO₄³⁻	20	50	- 100	- 330
As	10	20	10	- 10
Mn	750	1,620	1,330	10
Fe	1,180	3,360	960	260

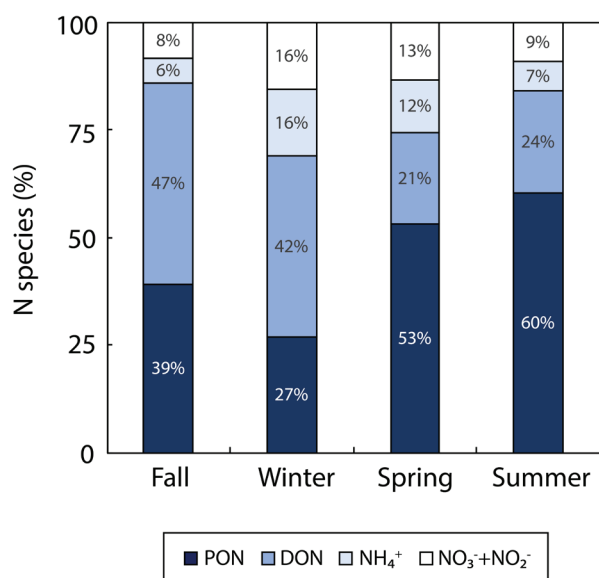


Figure 6 Relative proportion of individual N species as a percentage of the seasonal upscaled Delta-wide island drainage total nitrogen (TN) flux for WY 2018 (see text for details).

greater net positive fluxes during other seasons though, as indicated by the positive annual island drainage net fluxes for all constituents except PO_4^{3-} (Table 4).

DISCUSSION

Controls on Island Drainage Nutrient and Trace Element Composition

Nitrogen

The multi-species stable isotope data we collected provides new insight into the dominant biogeochemical processes that control N species concentrations and stable isotope composition in island drainage. The clear distinctions in $\delta^{15}\text{N}$ values of inorganic and organic N pools in drainage from all islands suggests that N is cycled in a relatively consistent biogeochemical manner across Delta islands (Figure 4). Similarity between $\delta^{15}\text{N}$ values of PON and DON indicates that DON is mainly derived from the breakdown of larger OM, such as PON. Drainage POM likely originates from soil as discussed by Richardson et al. (2020), which showed that annual mean (C:N)_m ratios of POM were generally above 10 at these sites. The higher $\delta^{15}\text{N}$ - NH_4^+ values in nearly all samples relative to $\delta^{15}\text{N}$ -PON and $\delta^{15}\text{N}$ -DON values suggests that the

stable isotope signature of mineralized organic N—which would have NH_4^+ with lower $\delta^{15}\text{N}$ - NH_4^+ values relative to its organic source—is overprinted by other biogeochemical processes common to all sites (Nadelhoffer and Fry 1994).

This unexpected elevation in $\delta^{15}\text{N}$ - NH_4^+ values relative to organic N pools is best explained by a combination of nitrification, uptake, and volatilization of NH_4^+ , all of which would lead to preferential loss of $^{14}\text{NH}_4^+$ and/or $^{14}\text{NH}_3$ that leaves remaining NH_4^+ enriched in ^{15}N (Ostrom et al. 1998; Clark 2015). The NH_4^+ pool is likely subject to uptake and volatilization in the unsaturated zone during summer and fall when water tables are low and plant biomass is high. The seasonality in NH_4^+ concentrations across all sites suggests that increases in NH_4^+ concentrations coincide with known winter and spring periods of water table rises from seasonal shifts in island hydrology (evapotranspiration, precipitation, etc.). As such, drainage outlets receive mineralized NH_4^+ that is mobilized and transported from shallow soil stores during winter and spring that was previously subjected to uptake and volatilization during the summer and fall. Some of the material transported during this time could be pulsed off-island as “first flush” events, but the sustained elevation in N content in drainage suggests that seasonal shifts in primary water sources are the major driver of change. Under oxic conditions, a portion of NH_4^+ can also be converted to NO_3^- via nitrification, which will also leave behind a ^{15}N -enriched NH_4^+ pool. The spatial and temporal variability in NO_3^- and NO_2^- concentrations along with $\delta^{15}\text{N}$ - NO_3^- values across all sites suggests that these processes change irregularly and are not spatially or temporally consistent.

Values of $\delta^{15}\text{N}$ - NO_3^- were generally low with lower NO_3^- concentration relative to the NH_4^+ pool, which is consistent with partial nitrification of NH_4^+ . Some of the NH_4^+ appears to be nitrified locally in the subsurface and/or in the drainage waters under sub-oxic to oxic conditions, possibly from hot spots and hot moments of NO_3^- and NO_2^- production (McClain et al. 2003). Additional inorganic N sources external to

the system were also evidenced by high $\delta^{15}\text{N-NO}_3^-$ values in several samples on Staten Island that overlapped or were higher than $\delta^{15}\text{N-NH}_4^+$ values. The high NO_3^- concentrations and $\delta^{15}\text{N-NO}_3^-$ values of these samples show the influence of a N input that is most consistent with a high-concentration, partially-denitrified fertilizer source (Kendall and McDonnell 2012; Clark 2015). We generated estimates of N fertilizer application amounts to each island using areal crop cover estimates and the N application rate associated with each crop, as available, from Rosenstock et al. (2013); these rates are not based on data from Delta islands and not all land cover types have N application rate data, so estimates are considered preliminary. Estimates of fertilizer inputs on Staten (~800,000 kg N) and Sherman (~230,000 kg N) islands eclipsed TDN gross fluxes by an order of magnitude, while Twitchell Island fertilizer application estimates were much smaller (~38,000 kg N). These estimates suggest that fertilizer N may be an important source of “new” island N annually, especially on cropland-dominated islands such as Staten Island. Importantly, the N stable isotope data generally suggests that any fertilizer N that leaves via drainage is generally highly recycled.

At the individual site level, N species stable isotope values were highly variable, both spatially and temporally (Table 1). Such variability in individual N species stable isotope values, without context relative to other N pools, shows that biogeochemical controls and sources are complex at small spatial and temporal scales. However, the clear distinctions among the N pools and stable isotope composition in island drainage as a whole show that there are indeed broad, common links in N cycling across Delta islands.

Silicon and Phosphorus

Concentrations of SiO_4^{4-} were seasonally elevated in the fall and winter in island drainage (Figure 3F) and suggestive of increased groundwater contributions in line with expected water table fluctuations (Richardson et al. 2020). This finding is not surprising because SiO_4^{4-} concentrations in groundwater are commonly high relative to those in river water

as a result of water-mineral interactions in the subsurface. In the case of island hydrology, mineral accumulation from evaporation may also contribute to higher SiO_4^{4-} in the subsurface. In contrast, controls on drainage PO_4^{3-} concentrations (Figure 3G) were not clear, although some sites showed higher concentrations in the summer, which may indicate that most PO_4^{3-} is sourced from fertilizer application during the growing season. Phosphorous is subject to complex sorption reactions in the subsurface that can significantly limit mobility, which may account for the generally low drainage PO_4^{3-} concentrations year-round (Schoumans 2013). Studies on fertilizer applications of soluble phosphorous show that over 50% of the added PO_4^{3-} is immobilized in under 3 days (do Nascimento et al. 2018).

Trace Elements

We found high concentrations of total dissolved Mn and Fe in island drainage during winter and spring months when compared to summer (Figure 3H and 3I). Mobilization of Fe and Mn in water is commonly associated with redox state, and the observed seasonal increases in total dissolved Fe and Mn concentrations suggest that drainage waters receive contributions from a reduced water source seasonally. This seasonality has been observed for other trace elements in temporarily flooded fields of the Delta, where re-wetting periods are thought to mobilize mercury species previously formed in unsaturated soils during dry phases (Marvin-DiPasquale et al. 2014). Regionally, reduction of Fe- and Mn-oxides commonly leads to increases in soluble Fe and Mn species in groundwater (Bennett et al. 2006). However, we found no relationship between total dissolved Fe and Mn concentrations across all sites, though site-specific trends were evident at some locations (but weakly correlated) (Figure 7). Interestingly, total dissolved Mn and DOC concentrations ($R^2=0.29$) were weakly positively correlated, while total dissolved Fe and dissolved oxygen concentrations ($R^2=0.38$) along with pH ($R^2=0.37$) were weakly negatively correlated when considering all sites (Figure 7). This dynamic relationship suggests that controls on total dissolved Mn and organic matter inputs may be

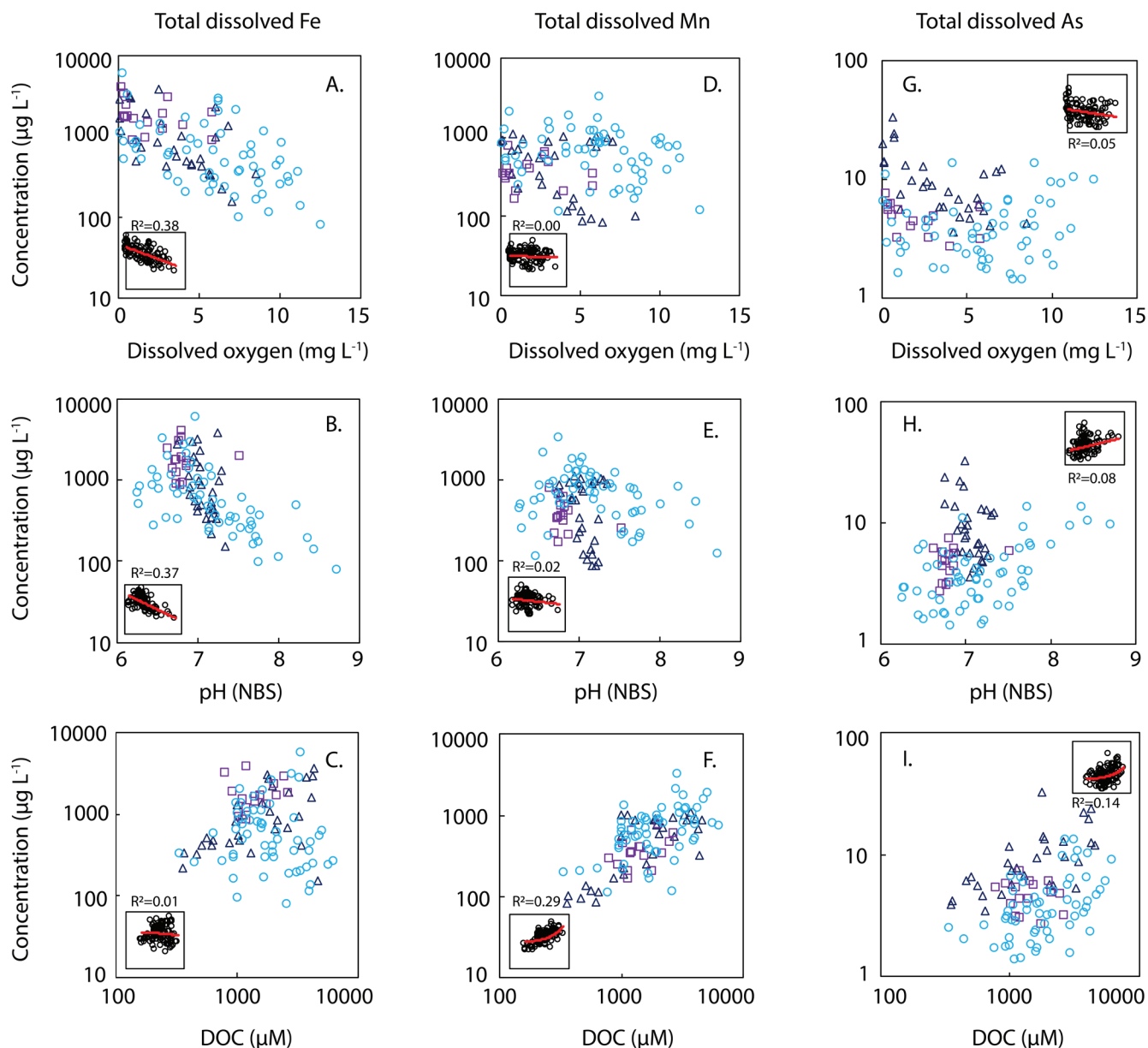


Figure 7 Island drainage total dissolved Fe, Mn, and As concentrations versus (A, D, G) dissolved oxygen, (B, E, H) pH, and (C, F, I) DOC concentration for all 16 months of sampling in WY 2017 and WY 2018. *Inset figures* show cumulative R^2 value for exponential regressions when considering all sites. *Light blue circles, dark blue triangles, and purple squares* represent drainage sites on Sherman, Staten, and Twitchell islands, respectively.

broadly related across all islands, which is not surprising given that organic matter has a high retention capacity for trace elements (Aiken et al. 2011). The negative relationship between total dissolved Fe and dissolved oxygen as well as pH, but lack of a relationship between total dissolved Fe and DOC, suggests that redox processes may

be a more important driver of Fe solubility and speciation than OM in drainage waters. Since island drainage integrates the effects of both solute source contributions and biogeochemical processes that change solubility and speciation, it is hard to assess the importance of each of these processes without detailed porewater studies.

Total dissolved As concentrations in island drainage were more variable than Fe and Mn, with no clear seasonal trends across sites (Figure 3J). Reduction of As-bearing Fe- and Mn-oxides is the primary mechanism for As contamination of groundwater in the Delta and areas nearby (e.g., northern San Joaquin Basin) (Izbicki et al. 2008; Bennett and Belitz 2010). In fact, some of the highest concentrations of acid-extractable As—a measure of As available for desorption from mineral surfaces—in this region are from Delta sediments (Izbicki et al. 2008). Similar to PO_4^{3-} , complex sorption reactions affect As mobilization (Herath et al. 2016), and the variability in As concentrations observed across sites in our study is likely a reflection of the complex As biogeochemistry in both the subsurface and surface waters of Delta islands. Broadly, total dissolved As concentrations in drainage were higher under low oxygen conditions, aside from a subset of samples collected on Sherman Island (Figure 7G). While reductive dissolution reasonably explains As mobilization under low oxygen conditions, this subset of Sherman Island samples may actually represent As mobilization from a different biogeochemical process. In high pH oxic waters, As can be mobilized via alkali desorption and sulfide oxidation (Herath et al. 2016).

Interestingly, drainage waters on Staten Island had mean annual dissolved As concentrations that were almost double the other drainage sites and, at times, exceeded recommended thresholds of total dissolved As set by the US Environmental Protection Agency (USEPA) ($> 10 \mu\text{g L}^{-1}$) and World Health Organization ($> 30 \mu\text{g L}^{-1}$). We suspect that these high levels of total dissolved As, which were specific to Staten Island, are related to seasonal flooding of fields that contribute to localized anoxic conditions. This is also evidenced by past studies showing large CH_4 fluxes during these times, that likely allow for release of As via reductive dissolution (Pellerin et al. 2013). Taken together, trace element geochemistry broadly suggests that island drainage receives water from a seasonally reduced water source or NRZ; future work could explicitly sample along possible flow paths to better account for differences

in source geochemistry and biogeochemical transformations during transport to drainage ditches (and ultimately surrounding river channels).

Island Drainage Nutrient and Trace Element Contributions to Delta Waterways

Sherman, Staten, and Twitchell islands were each a net annual source of TN, TDN, NH_4^+ , DON, PON, total dissolved Mn and Fe, and a net annual sink for SiO_4^{4-} and PO_4^{3-} (Table 2). Sherman and Twitchell islands were also sinks for $\text{NO}_3^- + \text{NO}_2^-$, while Staten Island was a net source of $\text{NO}_3^- + \text{NO}_2^-$ (Table 2). Upscaled to Delta-wide contributions, calculated mean annual island drainage gross TN fluxes were 7390 kg d^{-1} (or $2.7 \times 10^6 \text{ kg annually}$), and net TN fluxes were $5,030 \text{ kg d}^{-1}$ (or $1.8 \times 10^6 \text{ kg annually}$) (Table 3). This finding complicates many existing N box models in the Delta, which commonly assume island drainage N inputs are negligible or net zero (Novick et al. 2015). The net and gross annual island drainage TN load for WY 2018 was about 9% and 13%, respectively, of previously reported annual TN loads from the Sacramento River (including SRWTP) and San Joaquin River combined ($\sim 1.8 \times 10^7 \text{ kg}$) (Saleh and Domagalski 2015) (Table A6).

To further examine the relative importance of island drainage TN and NH_4^+ inputs, we revised three existing box models (“SFEI,” “DSM2,” and “EPA”) described in Novick et al. (2015) and TetraTech (2006) to include our new estimates of (1) island drainage TN and NH_4^+ fluxes off-island, and (2) river TN and NH_4^+ fluxes on-island (Table A6). We found that gross island drainage contributions could account for $\sim 13\%$ to 17% of annual TN loads into the Delta, while TN loads from river inflow onto islands could account for $\sim 8\%$ to 10% of TN flow out of Delta waters. These existing models also suggest that the Delta is a sink for NH_4^+ and TN that enters the region from riverine inputs. Taking island drainage inputs into account, we estimated whole-Delta TN losses of 33% to 35% , which is slightly higher in range than original estimates of 25% from Novick et al. (2015) and in close agreement with original estimates of 35% from TetraTech (2006) (Table A6). Our annual NH_4^+ losses in the Delta ranged from 64%

to 87% and were similar to past estimates of 65% to 85% from Novick et al. (2015). These revisions to existing box models to include island drainage loads from this study, which is a net source of both TN and NH_4^+ , suggests that the Delta is a slightly larger sink for TN ($+1.9 \times 10^5$ kg to 1.8×10^6 kg) and NH_4^+ ($+2.1 \times 10^5$ kg) than previous estimates suggest (Table A6).

In contrast to N dynamics, Delta islands were a net sink for PO_4^{3-} during WY 2018 (Table 3). The annual gross PO_4^{3-} load in drainage waters pumped off islands was 2.8×10^4 kg, which is similar in magnitude to past estimates of $\sim 5.1 \times 10^4$ kg (TetraTech 2006). However, island drainage exports of PO_4^{3-} were negated by the larger inflow of PO_4^{3-} onto islands, resulting in islands being a net sink for PO_4^{3-} to the order of -3.2×10^4 kg annually (Table 3). Relative to previously reported annual estimates of PO_4^{3-} inputs to the Delta, the gross island drainage PO_4^{3-} contribution comprised just 1% of existing PO_4^{3-} contributions to the Delta (TetraTech 2006).

Delta islands were, annually, a net source of total dissolved Mn (3.4×10^5 kg), Fe (5.3×10^5 kg), and As (2.3×10^3 kg) to the larger Delta environment (Table 3). Most of these loads likely precipitate in the Delta's oxic river waters and are deposited in the sediments. Similar to concerns about methylmercury in the Delta, re-suspension of sediments via dredging or other physicochemical processes could remobilize elements deposited from island drainage for downstream transport, with ultimate fate depending on concentrations and speciation (Shipley et al. 2011).

A large fraction of the previously discussed nutrient and trace element exports from Delta islands occurred in the winter and spring, from increases in both concentrations and discharge (Figure 3, Figure A1). Seasonality in the delivery of island drainage nutrients and trace elements to Delta waters has important implications for mass flux and net flux comparisons. For example, nearly 65% and 68% of the annual upscaled gross TN and TDN load, respectively, was delivered in winter and spring of WY 2018 (Table 4). Island drainage nutrient and trace element fluxes also

likely shift inter-annually from differences in island-level and Delta-wide hydrology. Inflow to outflow ratios at the island level were highly variable across islands and water years (Table A3, A4). Inflow and drainage constituent concentrations may also change year to year, and even slight changes could affect the magnitude of net fluxes. Richardson et al. (2020) estimated that wet water years see greater mass fluxes of carbon from island drainage, and these results may scale to N. Future work should consider the importance of water year variability, which can affect both concentrations and discharge, when estimating the relative contributions of different nutrient sources internal and external to the Delta. Seasonality also matters because the fate and effects of these inputs will vary with environmental conditions (e.g., flow, temperature, and solar radiation). For example, flows in the Delta are higher in the winter and spring, which may facilitate rapid transport and dilution through the system relative to other seasons. In the summer and fall, changes in nutrient concentrations and forms may be of greater consequence as they overlap with warmer temperatures and higher solar radiation that can promote phytoplankton growth.

Importance of Island Drainage Nutrient Contributions Using Pre- and Post-Upgrade SRWTP Scenarios

To better understand the relative magnitude of island drainage nutrient contributions in the context of the larger Delta environment under pre- and post-upgrade scenarios, we first compared island drainage nutrient contributions to other major Delta inflows (Sacramento and San Joaquin rivers) along with contributions from SRWTP, pre-upgrade, for WY 2018. We focus on dissolved N and P based on data availability from the above river sites and SRWTP. Annual net island drainage TDN, NH_4^+ , $\text{NO}_3^- + \text{NO}_2^-$, and PO_4^{3-} contributions were 7%, 4%, 2%, and -4% of total inputs to the Delta, respectively (Figure 8, Table A7). During WY 2018, SRWTP NH_4^+ contributions were 92% of all NH_4^+ inputs, and this mass flux percentage is nearly identical to past estimates by Jassby (2008). Seasonally, we estimated island drainage contributed around 16% of TDN, 9% of NH_4^+ , 10% of $\text{NO}_3^- + \text{NO}_2^-$, and

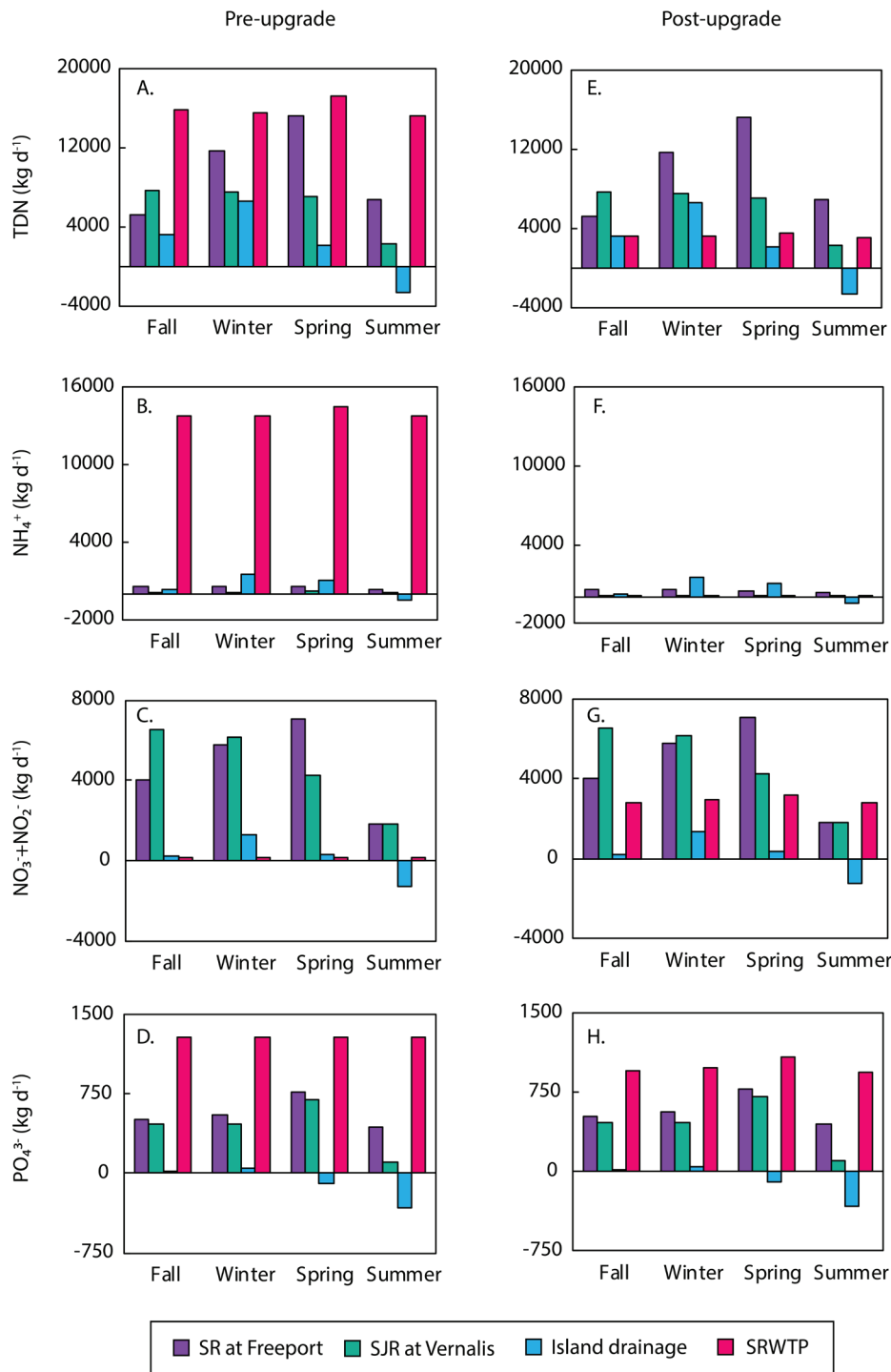


Figure 8 Calculated mean seasonal fluxes to the Delta from the Sacramento River (SR) at Freeport, the San Joaquin River (SJR) at Vernalis, Delta-wide island drainage (taken as net contributions), and Sacramento Regional Wastewater Treatment Plant (SRWTP) under (A-D) pre-upgrade and (E-H) post-upgrade conditions. Fluxes were calculated using flow and generally monthly concentration data from water year (WY) 2018. River sites had some months of missing data, depending on species, and, as such, we present these fluxes as baseline seasonal estimates for WY 2018, a dry year. Pre-upgrade PO₄³⁻ fluxes at SRWTP were calculated from three months (Oct-17 to Dec-17) of data in WY 2018 due to limited concentration data, and the decrease in PO₄³⁻ fluxes across upgrade scenarios for SRWTP is a residual effect of bias in the WY 2018 mean as SRWTP PO₄³⁻ fluxes are not expected to change significantly.

2% of PO_4^{3-} in winter months under pre-upgrade conditions (Table A7). In the summer and fall, net contributions from island drainage represented -12% and 10% of TDN, -3% and 2% of NH_4^+ , -47% and 2% of $\text{NO}_3^- + \text{NO}_2^-$, and -21% and -1% of PO_4^{3-} total inputs under pre-upgrade conditions (Table A7).

Predicted effluent $\text{NO}_3^- + \text{NO}_2^-$, NH_4^+ , PO_4^{3-} , and TDN concentrations for SRWTP—once fully upgraded to tertiary treatment with biological nutrient removal (i.e., nitrification and denitrification)—were used to forecast possible changes in dominant N and P sources to and within the Delta under a post-upgrade SRWTP scenario. Post-upgrade, annual net island drainage contributions were predicted to comprise 11% of the TDN, 45% of the NH_4^+ , and 1% of the $\text{NO}_3^- + \text{NO}_2^-$ delivered to and within the Delta relative to inputs from major inflows and SRWTP (Figure 8, Table A7). Since SRWTP does not anticipate changes to its PO_4^{3-} loads, net island drainage PO_4^{3-} percent contributions remained relatively similar, around -4% to -5%, under pre- and post-upgrade scenarios. Pre- versus post-upgrade seasonal percentages for winter net island drainage N contributions shifted from 16% to 23% for TDN, and from 9% to 65% for NH_4^+ , while $\text{NO}_3^- + \text{NO}_2^-$ percent contributions remained around 8% to 10% (Table A7).

Because overall NH_4^+ inputs to the Delta will be reduced as SRWTP transitions to be a more advanced treatment plant, following the upgrade, a large fraction of NH_4^+ that enters the Delta may originate internally from island drainage. Importantly, a majority of island drainage N delivery to Delta waterways will occur seasonally, in the winter and spring, when carbon and trace element contributions from drainage are similarly elevated (Richardson et al. 2020) (Figure 8, Table 4). Though NO_3^- will likely dominate external inorganic N loads to the Delta post-upgrade, the seasonal delivery of N from island drainage will be measurable and may be locally relevant. The spatially diffuse locations of drainage outfalls may mean that these seasonal loads are delivered to regions of the Delta with long residence times that allow for extended

biogeochemical processing and incorporation into the food web.

Study Limitations and Applications

This study is an important first step toward better constraining and evaluating the importance of island drainage nutrient contributions to the Delta. Future work should work toward resolving water budget uncertainties and issues relating to scale, both in space and time. Island water budgets, which are commonly modeled in this system, would benefit from ground truthing where possible. In the context of this study, explicit accounting of water inflow volumes could improve a source of uncertainty in both net flux estimates and island water budgets. Specifically, our study was limited by two key assumptions that warrant further work and improvement: (1) that island water budgets are at steady-state, and (2) that the regional estimates of island drainage from Templin and Cherry (1997) are accurate. The steady state water budget assumptions used herein affect the resulting mass flux estimates. A simple sensitivity analysis shows that changing inflow based on expected directional shifts in on-island water storage seasonally (decreases in spring/summer, increases in fall/winter) increases annual and seasonal net mass fluxes for nearly all constituents; many analytes become smaller sinks and/or larger sources, especially in the summer (Table A8). Additionally, if Delta-wide drainage outflow is closer to DCD estimates (2 times greater, $1.2 \cdot 10^9 \text{ m}^3$ for WY 2018), the mass flux estimates herein are clear underestimates.

High-frequency monitoring of drainage outlets—for nutrient concentrations and related ancillary water-quality parameters such as temperature, dissolved oxygen, and pH—could be used for better resolution of mass flux estimates and shifting nutrient biogeochemistry in island drainage. Similar recent work, enabled by deployment of high-frequency sensor networks, showed nutrient dynamics can change at time-scales of hours, days, and weeks in the Delta (Downing et al. 2017; Kraus et al. 2017), and we suspect a similar high-frequency data set for multiple island drainage sites could help resolve some of the variability seen in this study and

companion work by Richardson et al. (2020). Such monitoring would also likely generate more refined and accurate load estimates both within and across water years.

For more explicit source tracking, coupled physicochemical instrumentation (e.g., water level, chemical sensors) of island groundwater and drainage waters across multiple islands could provide a better understanding of biogeochemical transformations as they occur from initial diversion or infiltration to final discharge. Our use of stable isotope tracers provided new insight into N cycling on Delta islands and a similar application of isotopic tracers could be used in conjunction with the suggested monitoring regime to better understand N sources and transformations.

Beyond nutrients, work on contaminants in the Delta suggests farmed Delta islands may also be a source of a number of ecologically consequential pesticides, transported in dissolved forms and/or sorbed on soil particulates (Kuivila and Hladik 2008; De Parsia et al. 2019; Weston et al. 2019). With over 200 possible active drainage sites in this system, new studies could examine the possibility of delivery of these contaminants via island drains in the Delta. Drainage waters may also be a potential source for harmful algae and cyanotoxins that has not been studied; Richardson et al. (2020) found several island drainage sites had seasonal algal blooms.

Finally, this study and past work show that Delta islands are spatially heterogeneous, both within islands and across islands. This has been observed in studies of (1) gas fluxes, which can be remarkably variable across identical land-use types on multiple Delta islands (Hemes et al. 2019), and (2) aqueous fluxes of carbon, nutrients, and trace elements, with clear site-to-site variability in concentrations as shown in this study and Richardson et al. (2020). Better resolution of controls on this spatial heterogeneity—which affects system-wide assessments of gaseous, aqueous, and particulate fluxes—could provide more accurate upscaling of lateral and vertical fluxes. Similarly, identifying

how different land uses affect constituent source and sink dynamics could also help inform best management practices on Delta islands.

CONCLUSIONS

We estimated island-level and upscaled Sacramento-San Joaquin Delta (Delta)-wide drainage fluxes using monthly nutrient (PON, DON, $\text{NO}_3^- + \text{NO}_2^-$, NH_4^+ , PO_4^{3-} , SiO_4^{4-}) and trace element (total dissolved Fe, Mn, and As) concentrations with discharge data. Upscaled island drainage estimates for the entire Delta suggested that islands are annual net sources of total nitrogen (TN), total dissolved nitrogen (TDN), NH_4^+ , $\text{NO}_3^- + \text{NO}_2^-$, DON, PON, SiO_4^{4-} , total dissolved Mn, Fe, and As, and sinks for PO_4^{3-} . Island drainage net annual TN and TDN exports were 1.8×10^6 and 8.4×10^5 kg, respectively. Delta-wide island drainage gross and net TN contributions were roughly 13% and 9% of previously reported TN loads to the system. Our results complicate existing nutrient budgets in the Delta—which commonly assume that N inputs from island drainage are negligible or net zero—and provide new information on under-studied trace element inputs to the Delta.

Using forecasted changes in post-upgrade Sacramento Regional Wastewater Treatment Plant (SRWTP) dissolved N and P loads, we also estimated how relative contributions of N and P from island drainage and other major freshwater inflow sources could shift in importance in the Delta environment. Under a post-upgrade scenario, annual island drainage net TDN and NH_4^+ contributions to the Delta—relative to inputs from the San Joaquin River, the Sacramento River, and SRWTP—increased in relative importance from 7% to 11% and 4% to 45% based on data from 2018 (a dry water year), respectively. Both pre- and post-upgrade $\text{NO}_3^- + \text{NO}_2^-$ and PO_4^{3-} percent contributions from island drainage—relative to other considered sources—were similar, suggesting that the recent SRWTP upgrade, which reduces total N loads while maintaining similar P loads to the Delta, will also shift dominant sources of N species in different ways. Of these sources, island drainage may become

the dominant source of NH_4^+ to Delta waterways, at least during dry water years, though more work is needed to assess how NH_4^+ fluxes from other sources, like wetlands and sediments, may factor into the shifting N budget. Seasonal island drainage net TDN fluxes (2,140 to 6,600 kg d^{-1}) will also be similar in magnitude to post-upgrade TDN fluxes from SRWTP (3,110 to 3,530 kg d^{-1}) for most of the year (fall through spring). The increased role of island drainage nutrients may have implications for ecosystem dynamics, especially in places where drains empty into long residence time areas (sloughs, etc.) of the Delta.

More broadly, this work shows that island drainage is an existing and measurable source of nutrients and trace elements, at least during dry water years, and highlights the importance of accounting for temporal variability in existing nutrient budgets. Our understanding of dominant nutrient sources in the Delta may be biased without further consideration of mass fluxes as they relate to seasonal, annual, and interannual time-scales in a system with direct water year dependence that is projected to become even more variable in the coming years.

ACKNOWLEDGEMENTS

We thank the Nature Conservancy for their assistance in accessing sampling locations, and the California Department of Water Resources for helping arrange access to sampling locations. We thank Carol Kendall for her early support and assistance with this work. We thank Kaylee Glenney, Carolyn Brady, and Rob Franks for their help in the Marine Analytical Lab. This research was supported by grants from the International Association of Geochemistry, National Geographic, and the J. Casey Moore Award. Additional support for C. Richardson was provided by the National Science Foundation Graduate Research Fellowship Program (DGE-1329626), and J. Fackrell received support from the California Sea Grant Delta Science Fellowship (R/SF-84). Island drainage geochemistry and flow data is publicly available through HydroShare from the Consortium of Universities for the Advancement of Hydrologic

Science, Inc. (CUAHSI) at <http://www.hydroshare.org/resource/90464d9f9bb34c43b9c6b13eafb5e843>. Any use of trade, firm, or product names is for descriptive purposes only and does not imply endorsement by the US Government.

REFERENCES

- Aiken GR, H Hsu-Kim H, Ryan JN. 2011. Influence of dissolved organic matter on the environmental fate of metals, nanoparticles, and colloids. *Environ Sci Tech*. [accessed 2020 Jan 1]. <https://doi.org/10.1021/es103992s>
- Alpers CN, Fleck JA, Marvin-DiPasquale M, Stricker CA, Stephenson M, Taylor HE. 2014. Mercury cycling in agricultural and managed wetlands, Yolo Bypass, California: Spatial and seasonal variations in water quality. *Sci Total Environ*. [accessed 2020 Jan 1];484:276-287. <https://doi.org/10.1016/j.scitotenv.2013.10.096>
- Bachand PA, Bachand SM, Kraus TEC, Stern D, Liang YL, Horwath WR. 2019. Sequestration and transformation in chemically enhanced treatment wetlands: DOCs, DBPPs, and nutrients. *J Environ Eng*. [accessed 2020 Jan 1];145(8), 04019044. [https://doi.org/10.1061/\(ASCE\)EE.1943-7870.0001536](https://doi.org/10.1061/(ASCE)EE.1943-7870.0001536)
- Bennett GL, Belitz K. 2010. Groundwater quality in the Northern San Joaquin Valley, California. US Geological Survey Fact Sheet 2010-3079. [accessed 2020 Jan 1]. 4 p. <https://doi.org/10.3133/fs20103079>
- Bennett GL, Belitz K, Milby Dawson BH. 2006. California GAMA Program—ground-water quality data in the northern San Joaquin basin study unit. Sacramento (CA): US Geological Survey. Data Series 196. [accessed 2020 Jan 1]. 122 p. Available from: <https://pubs.usgs.gov/ds/2006/196/> [CDWR] California Department of Water Resources. 1995. Sacramento-San Joaquin Delta Atlas: State of California. [accessed 2020 Jan 1]. 121 p. Available from: <https://cawaterlibrary.net/document/sacramento-san-joaquin-delta-atlas/>
- Clark I. 2015. Groundwater geochemistry and isotopes. New York (NY): CRC Press. 402 p.
- Cloern JE. 2019. Patterns, pace, and processes of water-quality variability in a long-studied estuary. *Limnol Oceanogr*. [accessed 2020 Jan 1];64(S1):S192-S208. <https://doi.org/10.1002/lno.10958>

- Cloern JE. 2021. Use care when interpreting correlations: the ammonium example in the San Francisco Estuary. *San Franc Estuary Watershed Sci.* [accessed 2020 Jan 1];19(4).
<https://doi.org/10.15447/sfew.2021v19iss4art1>
- Dahm C, Parker A, Adelson A, Christman M, Bergamaschi B. 2016. Nutrient dynamics of the Delta: effects on primary producers. *San Franc Estuary Watershed Sci.* [accessed 2020 Jan 1];14(4).
<https://doi.org/10.15447/sfew.2016v14iss4art4>
- De Parsia M, Woodward EE, Orlando JL, Hladik ML. 2019. Pesticide mixtures in the Sacramento–San Joaquin Delta, 2016–17: results from Year 2 of the Delta Regional Monitoring Program. [accessed 2020 Jan 1]. <https://doi.org/10.3133/ds1120>
- Deverel SJ, Leighton DA. 2010. Historic, recent, and future subsidence, Sacramento-San Joaquin Delta, California, USA. *San Franc Estuary Watershed Sci.* [accessed 2020 Jan 1];8(2).
<https://doi.org/10.15447/sfew.2010v8iss2art1>
- Deverel SJ, Lucero CE, Bachand S. 2015. Evolution of arability and land use, Sacramento–San Joaquin Delta, California. *San Franc Estuary Watershed Sci.* [accessed 2020 Jan 1];13(2).
<https://doi.org/10.15447/sfew.2015v13iss2art4>
- Deverel SJ, Ingrum T, Leighton D. 2016. Present-day oxidative subsidence of organic soils and mitigation in the Sacramento-San Joaquin Delta, California, USA. *Hydrogeology.* [accessed 2020 Jan 1];24(3):569–586.
<https://doi.org/10.1007/s10040-016-1391-1>
- Diamond J, Williamson A. 1983. A summary of ground-water pumpage in the Central Valley of California. 1961-1977. US Geological Survey Water-Resources Investigations Report 83-4037. [accessed 2020 Jan 1]. 70 p. Available from:
<https://pubs.er.usgs.gov/publication/wri834037>
- do Nascimento CA, Pagliari PH, Faria Lda, Vitti GC. 2018. Phosphorus mobility and behavior in soils treated with calcium, ammonium, and magnesium phosphates. *Soil Sci Soc Am J.* [accessed 2020 Jan 1];82(3):622–631.
<https://doi.org/10.2136/sssaj2017.06.0211>
- Downing BD, Bergamaschi BA, Kraus TEC. 2017. Synthesis of data from high-frequency nutrient and associated biogeochemical monitoring for the Sacramento–San Joaquin Delta, northern California. US Geological Survey Scientific Investigations Report 2017–5066. [accessed 2020 Jan 1]. 28 p. <https://doi.org/10.3133/sir20175066>
- Du Laing, G, Rinklebe J, Vandecasteele B, Meers E, Tack FM. 2009. Trace metal behaviour in estuarine and riverine floodplain soils and sediments: a review. *Sci Total Environ.* [accessed 2020 Jan 1];407(13):3972–3985.
<https://doi.org/10.1016/j.scitotenv.2008.07.025>
- Dugdale R, Wilkerson F, Parker AE. 2015. The “ammonium paradox”: a summary of more than a decade of research into phytoplankton processes and nitrogen relationships in the northern San Francisco Estuary. Suisun Synthesis II Report Section 2. Prepared for the San Francisco Bay Nutrient Management Strategy. [accessed 2020 Jan 1]. Available from: https://bacwa.org/wp-content/uploads/2016/11/SuisunSynthesis2_November2016_DRAFT.pdf
- Glibert PM, Wilkerson FP, Dugdale RC, Raven JA, Dupont CL, Leavitt PR, Parker AE, Burkholder JM, Kana TM. 2016. Pluses and minuses of ammonium and nitrate uptake and assimilation by phytoplankton and implications for productivity and community composition, with emphasis on nitrogen-enriched conditions. *Limnol Oceanogr.* [accessed 2020 Jan 1];61(1):165–197.
<https://doi.org/10.1002/lno.10203>
- Hemes KS, Chamberlain SD, Eichelmann E, Anthony T, Valach A, Kasak K, Szutu D, Verfaillie J, Silver WL, Baldocchi DD. 2019. Assessing the carbon and climate benefit of restoring degraded agricultural peat soils to managed wetlands. *Agric For Meteorol.* [accessed 2020 Jan 1];268:202–214.
<https://doi.org/10.1016/j.agrformet.2019.01.017>
- Herath I, Vithanage M, Bundschuh J, Maity JP, Bhattacharya P. 2016. Natural arsenic in global groundwaters: distribution and geochemical triggers for mobilization. *Curr Pollut Rep.* [accessed 2020 Jan 1];2(1):68–89.
<https://doi.org/10.1007/s40726-016-0028-2>

- Hernes PJ, Dyda RY, Bergamaschi BA. 2020. Reassessing particulate organic carbon dynamics in the highly disturbed San Francisco Bay Estuary. *Front Earth Sci.* [accessed 2020 Jan 1];8:185. <https://doi.org/10.3389/feart.2020.00185>
- Howarth RF, Chan F, Conley DJ, Garnier J, Doney SC, Marino R, Billen G. 2011. Coupled biogeochemical cycles: eutrophication and hypoxia in temperate estuaries and coastal marine ecosystems. *Front Ecol Environ.* [accessed 2020 Jan 1];9(1):18-26. <https://doi.org/10.1890/100008>
- Izbicki JA, Stamos C, Metzger LF, Kulp T, McPherson KR, Halford K, Bennett GL. 2008. Sources, distribution, and management of arsenic in water from wells, Eastern San Joaquin ground-water subbasin, California. US Geological Survey Open-File Report 2008-1272. [accessed 2020 Jan 1]. 8 p. <https://doi.org/10.3133/ofr20081272>
- Jassby AD. 2008. Phytoplankton in the upper San Francisco Estuary: recent biomass trends, their causes, and their trophic significance. *San Franc Estuary Watershed Sci.* [accessed 2020 Jan 1];6(1). <https://doi.org/sfew.2008v6iss1art2>
- Jassby AD, Cloern JE. 2000. Organic matter sources and rehabilitation of the Sacramento-San Joaquin Delta (California, USA). *Aquat Conserv: Mar Freshw Ecosyst.* [accessed 2020 Jan 1];10(5):323-352. [https://doi.org/10.1002/1099-0755\(200009/10\)10:5<323::AID-AQC417>3.0.CO;2-J](https://doi.org/10.1002/1099-0755(200009/10)10:5<323::AID-AQC417>3.0.CO;2-J)
- Jassby AD, Cloern JE, Cole BE. 2002. Annual primary production: patterns and mechanisms of change in a nutrient-rich tidal ecosystem. *Limnol. Oceanogr.* [accessed 2020 Jan 1];47(3):698-712. <https://doi.org/10.4319/lo.2002.47.3.0698>
- Kendall C, McDonnell JJ. 2012. Isotope tracers in catchment hydrology. 2017. An introduction to high-frequency nutrient and biogeochemical monitoring for the Sacramento-San Joaquin Delta, northern California. [accessed 2020 Jan 1]. Elsevier <https://doi.org/10.3133/sir20175071>.
- Kraus TEC, Carpenter K, Bergamaschi B, Parker A, Stumpner E, Downing BD, Travis N, Wilkerson F, Kendall C, Mussen T. 2017. A river-scale Lagrangian experiment examining controls on phytoplankton dynamics in the presence and absence of treated wastewater effluent high in ammonium. *Limnol Oceanogr.* [accessed 2020 Jan 1];62(3):1234-1253. <https://doi.org/10.1002/lno.10497>
- Kuivila K, Hladik M. 2008. Understanding the occurrence and transport of current-use pesticides in the San Francisco estuary watershed. *San Franc Estuary Watershed Sci.* [accessed 2020 Jan 1];6(3). <https://doi.org/10.15447/sfew.2008v6iss3art2>
- Lehman P, Marr K, Boyer G, Acuna S, Teh SJJH. 2013. Long-term trends and causal factors associated with *Microcystis* abundance and toxicity in San Francisco Estuary and implications for climate change impacts. *Hydrobiologia.* [accessed 2020 Jan 1];718(1):141-158. <https://doi.org/10.1007/s10750-013-1612-8>
- Limpens J, Berendse F, Blodau C, Canadell J, Freeman C, Holden J, Roulet N, Rydin H, Schaepman-Strub G. 2008. Peatlands and the carbon cycle: from local processes to global implications: a synthesis. *Biogeosciences.* [accessed 2020 Jan 1];5(5):1475-1491. <https://doi.org/10.5194/bg-5-1475-2008>
- [LWA] Larry Walker Associates]. 2014. EchoWater Project EIR Water Quality Technical Memorandum. [accessed 2020 Jan 1].
- Marvin-DiPasquale M, Windham-Myers L, Agee JL, Kakouros E, Kieu LH, Fleck JA, Alpers CN, Stricker CA. 2014. Methylmercury production in sediment from agricultural and non-agricultural wetlands in the Yolo Bypass, California, USA. *Sci Total Environ.* [accessed 2020 Jan 1];48:288-299. <https://doi.org/10.1016/j.scitotenv.2013.09.098>
- McClain ME, Boyer EW, Dent CL, Gergel SE, Grimm NB, Groffman PM, Hart SC, Harvey JW, Johnston CA, Mayorga E. 2003. Biogeochemical hot spots and hot moments at the interface of terrestrial and aquatic ecosystems. *Ecosystems.* [accessed 2020 Jan 1];6:301-312. <https://doi.org/10.1007/s10021-003-0161-9>
- Murrell M, Hollibaugh J. 2000. Distribution and composition of dissolved and particulate organic carbon in northern San Francisco Bay during low flow conditions. *Estuar Coast Shelf Sci.* [accessed 2020 Jan 1];51(1):75-90. <https://doi.org/10.1006/ecss.2000.0639>
- Nadelhoffer KJ, Fry B. 1994. Nitrogen isotope studies in forest ecosystems. In: Lajtha K, Michner R (editors). *Stable isotopes in ecology and environmental science.* [accessed 2020 Jan 1]. 22-45 p.

- Novick E, Holleman R, Jabusch T, Sun J, Trowbridge P, Senn D, Guerin M, Kendall C, Young M, Peek M. 2015. Characterizing and quantifying nutrient sources, sinks and transformations in the Delta: synthesis, modeling, and recommendations for monitoring. SFEI Contribution No. 785. Richmond (CA): San Francisco Estuary Institute. [accessed 2020 Jan 1]. Available from: <https://www.sfei.org/documents/delta-nutrient-sources>
- Ogilbee W. 1966. Progress report - Methods for estimating ground-water withdrawals in Madera County, California. US Geological Survey Open-File Report. [accessed 2020 Jan 1]. 42 p. Available from: <https://pubs.usgs.gov/wri/1989/4107/report.pdf>
- Ogilbee W, Mitten. H 1970. A continuing program for estimating ground-water pumpage in California—Methods. US Geological Survey Open-File Report 70-246. 22 p. [accessed 2020 Jan 1]. Available from: <https://pubs.er.usgs.gov/publication/ofr70246>
- Ostrom NE, Knoke KE, Hedin LO, Robertson GP, Smucker AJ. 1998. Temporal trends in nitrogen isotope values of nitrate leaching from an agricultural soil. *Chem Geol.* [accessed 2020 Jan 1];146(3-4):219-227. [https://doi.org/10.1016/S0009-2541\(98\)00012-6](https://doi.org/10.1016/S0009-2541(98)00012-6)
- Paerl HW, Pinckney JL, Fear JM, Peierls BL. 1998. Ecosystem responses to internal and watershed organic matter loading: consequences for hypoxia in the eutrophying Neuse River Estuary, North Carolina, USA. *Mar Ecol Prog Ser.* [accessed 2020 Jan 1];166:17-25.
- Paerl HW, Valdes LM, Peierls BL, Adolf JE, Harding LJ. 2006. Anthropogenic and climatic influences on the eutrophication of large estuarine ecosystems. *Limnol Oceanogr.* [accessed 2020 Jan 1];51:448-462. https://doi.org/10.4319/lo.2006.51.1_part_2.0448
- Pellerin B, Anderson F, Bergamaschi B. 2013. Assessing the role of winter flooding on baseline greenhouse gas fluxes from corn fields in the Sacramento-San Joaquin Bay Delta. Energy Research and Development Division, Final Project Report. A report prepared for the California Energy Commission. [accessed 2020 Jan 1].
- Richardson C, Fackrell J, Kraus TEC, Young M, Paytan A. 2020. Lateral carbon exports from drained peatlands: an understudied carbon pathway in the Sacramento-San Joaquin Delta, California. *J Geophys Res Biogeosci.* [accessed 2020 Jan 1];125. <https://doi.org/10.1029/2020JG005883>
- Rosenstock TS, Liptzin K, Six J, Tomich TP. 2013. Nitrogen fertilizer use in California: assessing the data, trends and a way forward. *Calif Agric.* [accessed 2020 Jan 1];67(1).
- Saleh D, Domagalski J. 2015. SPARROW modeling of nitrogen sources and transport in rivers and streams of California and adjacent states, US. *J Am Water Resour Assoc.* [accessed 2020 Jan 1];51(6):1487-1507. <https://doi.org/10.1111/1752-1688.12325>
- Schoumans OF. 2013. Description of the phosphorus sorption and desorption processes in lowland peaty clay soils. *Soil Sci.* [accessed 2020 Jan 1];178(6):291-300. <https://doi.org/10.1097/SS.0b013e31829ef054>
- Seitzinger S, Sanders R. 1997. Contribution of dissolved organic nitrogen from rivers to estuarine eutrophication. *Mar Ecol Prog Ser.* [accessed 2020 Jan 1];159:1-12.
- Senn D, Novick E. 2014. Suisun Bay Ammonium synthesis report. Richmond (CA): San Francisco Estuary Institute. SFEI Contribution No. 706. p 191. [accessed 2020 Jan 1]. Available from: <https://www.sfei.org/documents/suisun-bay-ammonium-synthesis>
- Shipley HJ, Gao Y, Kan AT, Tomson MB 2011. Mobilization of trace metals and inorganic compounds during resuspension of anoxic sediments from Trepangier Bayou, Louisiana. *J Environ Qual.* [accessed 2020 Jan 1];40(2):484-491. <https://doi.org/10.2134/jeq2009.0124>
- Siegfried LJ, Fleenor WE, Lund JR. 2014. Physically based modeling of Delta Island consumptive use: Fabian Tract and Staten Island, California. *San Franc Estuary Watershed Sci.* [accessed 2020 Jan 1];12(4). <https://doi.org/10.15447/sfews.2014v12iss4art2>
- Sommer T, Armor C, Baxter R, Breuer R, Brown L, Chotkowski M, Culberson S, Feyrer F, Gingras M, Herbold B. 2007. The collapse of pelagic fishes in the upper San Francisco Estuary. *Fisheries.* [accessed 2020 Jan 1];32(6):270-277. [https://doi.org/10.1577/1548-8446\(2007\)32\[270:TCOPFI\]2.0.CO;2](https://doi.org/10.1577/1548-8446(2007)32[270:TCOPFI]2.0.CO;2)

- Stumpner EB, Kraus TEC, Fleck JA, Hansen AM, Bachand SM, Horwath WR, DeWild JF, Krabbenhoft DP, Bachand PA. 2015. Mercury, monomethyl mercury, and dissolved organic carbon concentrations in surface water entering and exiting constructed wetlands treated with metal-based coagulants, Twitchell Island, California. Data Series 950. [Reston (VA)]: US Geological Survey. 26 p. [accessed 2020 Jan 1];26. <https://doi.org/10.3133/ds950>
- Ta J, Anderson LW, Christman MA, Khanna, S, Kratville D, Madsen JD, Moran PJ, Viers JH. 2017. Invasive aquatic vegetation management in the Sacramento–San Joaquin River Delta: status and recommendations. *San Franc Estuary Watershed Sci.* [accessed 2020 Jan 1];15(4). <https://doi.org/10.15447/sfew.2017v15iss4art5>
- Templin WE, Cherry DE. 1997. Drainage-return, surface-water withdrawal, and land-use data for the Sacramento-San Joaquin Delta, with emphasis on Twitchell Island, California. US Geological Survey Open-file Report 97-350. [accessed 2020 Jan 1]. 31 p. <https://doi.org/10.3133/ofr97350>
- Tetra Tech, Inc. 2006. Conceptual model for nutrients in the Central Valley and Sacramento-San Joaquin Delta. A technical report prepared for the US Environmental Protection Agency and the Central Valley Drinking Water Public Policy Workgroup. [accessed 2020 Jan 1]. Available from: https://www.waterboards.ca.gov/centralvalley/water_issues/drinking_water_policy/final_nutrient_report_lowres.pdf
- [USGS] United States Geological Survey. 2019. National Water Information System: US Geological Survey Web Interface. [accessed 2020 Jan 1]. Available from: <https://doi.org/10.5066/F7P55KJN>
- Ward AK, Paerl HW. 2016. Delta nutrients forms and ratios public workshop: “Role of nutrients in shifts in phytoplankton abundance and species composition in the Sacramento-San Joaquin Delta.” Sacramento (CA): November 29-30, 2016. [accessed 2020 Jan 1]. Available from: https://www.waterboards.ca.gov/centralvalley/water_issues/delta_water_quality/delta_nutrient_research_plan/science_work_groups/2017_0530_phyto_wp.pdf
- Weston DP, Moschet C, Young TM, Johanif N, Poynton HC, Major KM, Connon RE, Hasenbein S. 2019. Chemical and toxicological effects on Cache Slough after storm-driven contaminant inputs. *San Franc Estuary Watershed Sci.* [accessed 2020 Jan 1];17(3). <https://doi.org/10.15447/sfew.2019v17iss3art3>
- Winder M, Jassby A. 2011. Shifts in zooplankton community structure: implications for food web processes in the upper San Francisco Estuary. *Estuaries Coasts.* [accessed 2020 Jan 1];34(4):675-690. <https://doi.org/10.1007/s12237-010-9342-x>
- Yabusaki SB, Wilkins MJ, Fang Y, Williams KH, Arora B, Bargar J, Beller HR, Bouskill NJ, Brodie EL, Christensen JN, et al. 2017. Water table dynamics and biogeochemical cycling in a shallow, variably-saturated floodplain. *Environ Sci Tech.* [accessed 2020 Jan 1];51(6):3307-3317. <https://doi.org/10.1021/acs.est.6b04873>

NOTES

- Liang L. 2020. Email communication between C. Richardson and Lan Liang, California Department of Water Resources, regarding island discharge comparisons in the Delta in July 2020.